(12) INTERNATIONAL APPLICATION PUBLISHED UNDER THE PATENT COOPERATION TREATY (PCT)

(19) World Intellectual Property Organization
International Bureau

(43) International Publication Date
27 June 2024 (27.06.2024)

WIPO | PCT

(10) International Publication Number
WO 2024/137614 A2

(51) International Patent Classification:
C25B 1/04 (2021.01)

(21) International Application Number:
PCT/US2023/084796

(22) International Filing Date:
19 December 2023 (19.12.2023)

(25) Filing Language: English

(26) Publication Language: English

(30) Priority Data:
63/433,746 19 December 2022 (19.12.2022) US

(71) Applicant: **THE REGENTS OF THE UNIVERSITY OF MICHIGAN** [US/US]; 1600 Huron Parkway, 2nd Floor, Ann Arbor, Michigan 48109 (US).

(72) Inventors; and

(71) Applicants: **YANG, Ke** [US/US]; 1600 Huron Parkway, 2nd Floor, Ann Arbor, Michigan 48109 (US). **BATISTA, Victor S.** [US/US]; 1600 Huron Parkway, 2nd Floor, Ann Arbor, Michigan 48109 (US).

(72) Inventors: **DONG, Wan Jae**; 1600 Huron Parkway, 2nd Floor, Ann Arbor, Michigan 48109 (US). **XIAO, Yixin**; 1600 Huron Parkway, 2nd Floor, Ann Arbor, Michigan 48109 (US). **MI, Zetian**; 1600 Huron Parkway, 2nd Floor, Ann Arbor, Michigan 48109 (US).

(74) Agent: **BRAIDWOOD, G. Christopher**; Lempia Summerfield Katz LLC, 20 South Clark Street, Suite 600, Chicago, Illinois 60603 (US).

(81) Designated States *(unless otherwise indicated, for every kind of national protection available)*: AE, AG, AL, AM, AO, AT, AU, AZ, BA, BB, BG, BH, BN, BR, BW, BY, BZ, CA, CH, CL, CN, CO, CR, CU, CV, CZ, DE, DJ, DK, DM, DO, DZ, EC, EE, EG, ES, FI, GB, GD, GE, GH, GM, GT, HN, HR, HU, ID, IL, IN, IQ, IR, IS, IT, JM, JO, JP, KE, KG, KH, KN, KP, KR, KW, KZ, LA, LC, LK, LR, LS, LU, LY, MA, MD, MG, MK, MN, MU, MW, MX, MY, MZ, NA, NG, NI, NO, NZ, OM, PA, PE, PG, PH, PL, PT, QA, RO, RS, RU, RW, SA, SC, SD, SE, SG, SK, SL, ST, SV, SY, TH, TJ, TM, TN, TR, TT, TZ, UA, UG, US, UZ, VC, VN, WS, ZA, ZM, ZW.

(54) **Title:** HYDROGEN PRODUCTION VIA SEAWATER SPLITTING

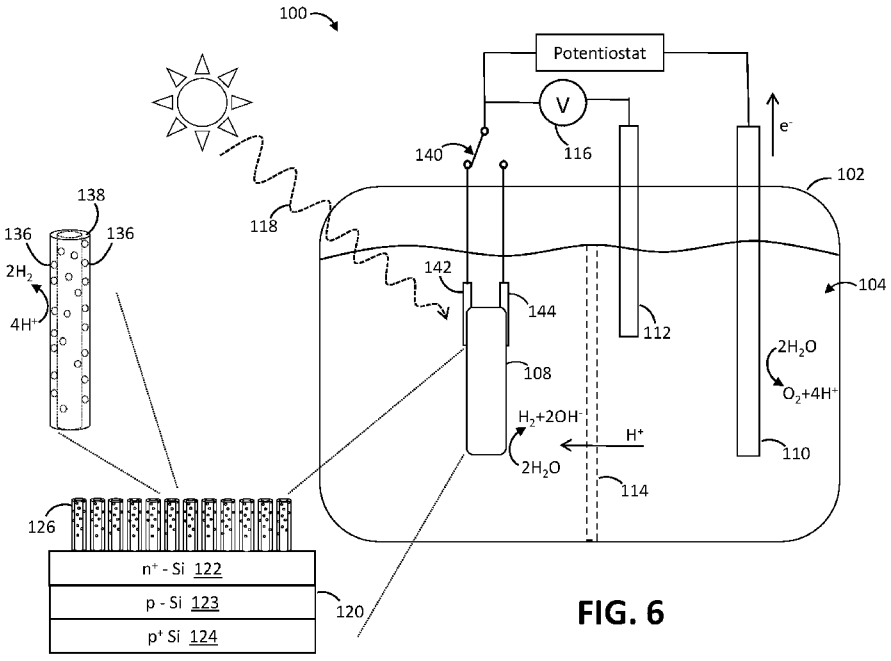

FIG. 6

(57) **Abstract:** A method of hydrogen production includes providing a solution and immersing a device in the solution. The device includes a substrate having a surface, an array of conductive projections supported by the substrate and extending outward from the surface of the substrate, and a plurality of catalyst nanoparticles disposed over the array of conductive projections. The solution includes dissolved sodium chloride (NaCl).

[Continued on next page]

WO 2024/137614 A2

(84) Designated States *(unless otherwise indicated, for every kind of regional protection available)*: ARIPO (BW, CV, GH, GM, KE, LR, LS, MW, MZ, NA, RW, SC, SD, SL, ST, SZ, TZ, UG, ZM, ZW), Eurasian (AM, AZ, BY, KG, KZ, RU, TJ, TM), European (AL, AT, BE, BG, CH, CY, CZ, DE, DK, EE, ES, FI, FR, GB, GR, HR, HU, IE, IS, IT, LT, LU, LV, MC, ME, MK, MT, NL, NO, PL, PT, RO, RS, SE, SI, SK, SM, TR), OAPI (BF, BJ, CF, CG, CI, CM, GA, GN, GQ, GW, KM, ML, MR, NE, SN, TD, TG).

Published:

— *without international search report and to be republished upon receipt of that report (Rule 48.2(g))*

HYDROGEN PRODUCTION VIA SEAWATER SPLITTING

CROSS-REFERENCE TO RELATED APPLICATION

[0001] This application claims the benefit of U.S. provisional application entitled "Hydrogen Production via Seawater Splitting," filed December 19, 2022, and assigned Serial No. 63/433,746, the entire disclosure of which is hereby expressly incorporated by reference.

STATEMENT REGARDING FEDERALLY SPONSORED RESEARCH OR DEVELOPMENT

[0002] This invention was made with government support under Grant No. W911NF-21-1-0337 awarded by the U.S. Army Research Office. The government has certain rights in the invention.

BACKGROUND OF THE DISCLOSURE

Field of the Disclosure

[0003] The disclosure relates generally to photoelectrodes, photocatalytic devices, and other devices for hydrogen evolution via water splitting and/or other reactions.

Brief Description of Related Technology

[0004] Hydrogen is a clean energy carrier that can replace fossil fuels due to its sufficiently high energy density and zero-carbon emission. Among several possible methods, water electrolysis has been proposed as one of the most promising routes to produce high-purity H_2 at low temperature. A sustainable and green hydrogen economy could be realized by water electrolysis powered by renewable energy using seawater as an earth-abundant hydrogen source. Acidic seawater, prepared by mixing an acid electrolyte with seawater, is an attractive aqueous solution for a highly efficient hydrogen evolution reaction (HER) because the concentration of protons near the cathode is very high. However, in acidic seawater, the competition with both the chloride oxidation reaction (COR) and the oxygen evolution reaction (OER) is inevitable at the anode. The COR is kinetically favored (although thermodynamically unfavored) when compared to the OER so the sluggish 4-electron kinetics of the OER leads to low O_2 selectivity. The difference between the standard

electrode potentials of the OER and COR can be gradually increased to 0.48 V by increasing the pH to up to 7.5. So, the COR could be suppressed under alkaline conditions.

[0005] Electrocatalysts have been developed for H_2 production by alkaline seawater splitting. However, under alkaline conditions with pH greater than about 9.5, the high concentration of OH^- ions can lead to precipitation of insoluble salts (*e.g.,* $Mg(OH)_2$ and $Ca(OH)_2$). A viable approach to address the drawbacks of acidic and alkaline seawater is to employ neutral or weak-alkaline ($7.5 < pH < 9.5$) seawater. In neutral electrolytes, the kinetic bottleneck of the low HER activity is due to the Volmer step of water dissociation ($H_2O + e^- \rightarrow H^* + OH^-$). In this regard, various electrocatalysts have addressed the H–OH cleavage in water molecules to enhance the HER under low overpotential. However, the HER activity in neutral-pH seawater is still behind that in the acidic and alkaline electrolytes.

[0006] Compared to the electrochemical method, photoelectrochemical (PEC) water splitting can achieve more efficient H_2 evolution by integrating semiconductor and co-catalytic materials. An electrical bias (*e.g.*, from a solar cell) can positively shift the onset potential and promote hydrogen evolution with less electrical power consumption. In the past decades, many semiconductor materials have been developed and applied as photocathodes for solar water splitting. However, conventional semiconductor materials such as Si, GaAs, and InP are easily corroded by surface holes accumulated under light illumination even in freshwater. The stability of such semiconductors further deteriorates in seawater due to strong oxidants (*e.g.*, chorine and hypochlorite). Although protective films on photoelectrodes have improved the stability in freshwater, to date, there have been a limited number of photocathodes that efficiently work in seawater.

SUMMARY OF THE DISCLOSURE

[0007] In accordance with one aspect of the disclosure, a method of hydrogen production includes providing a solution and immersing a device in the solution, the device including a substrate having a surface, an array of conductive projections supported by the substrate and extending outward from the surface of the substrate, and a plurality of catalyst nanoparticles disposed over the array of conductive projections. The solution includes dissolved sodium chloride (NaCl).

[0008] In accordance with another aspect of the disclosure, a device includes a substrate having a surface and a backside opposite the surface, an array of conductive projections supported by the substrate and extending outward from the surface of the substrate, a

plurality of catalyst nanoparticles disposed over the array of conductive projections, a first contact coupled to the backside and to which charge carriers photogenerated in the substrate in a photoelectrochemical (PEC) operational mode of the device move, and a second contact coupled to the array of conductive projections to provide charge carriers to the array of conductive projections in an electrochemical (EC) operational mode of the device.

[0009] In accordance with yet another aspect of the disclosure, a device includes a substrate having a surface, an array of conductive projections supported by the substrate and extending outward from the surface of the substrate, each conductive projection of the array of conductive projections including a metal-nitride semiconductor material, and a plurality of metal catalysts disposed over the array of conductive projections such that metal/metal-nitride interfaces are established. The metal/metal-nitride interfaces are configured to promote hydrogen production via water splitting.

[0010] In accordance with still another aspect of the disclosure, a method of fabricating a hydrogen production device includes providing a substrate having a surface, growing an array of nanowires on the surface of the substrate such that each nanowire of the array of nanowires extends outward from the surface of the substrate, each conductive projection of the array of conductive projections including a metal-nitride semiconductor material, and depositing a plurality of metal catalyst nanoparticles across the array of nanowires such that metal/metal-nitride interfaces are established, the metal/metal-nitride interfaces being configured to promote hydrogen production via water splitting.

[0011] In connection with any one of the aforementioned aspects, the devices and/or methods described herein may alternatively or additionally include or involve any combination of one or more of the following aspects or features. The solution includes seawater. The solution is a phosphate-buffered solution. Providing the solution includes lowering the pH of the solution. The method further includes illuminating the device such that charge carriers are photogenerated in the device to support the hydrogen production. Illuminating the device includes irradiating a backside of the substrate of the device with sunlight. The method further includes applying a bias voltage to the device. The device includes a contact coupled to a backside of the substrate. Applying the bias voltage includes applying the bias voltage to the contact in a photoelectrochemical (PEC) operational mode of the device. The method further includes, when the device is not illuminated, switching the bias voltage to apply the bias voltage to the array of conductive projections in an electrochemical operational mode of the device. The device includes a

eutectic alloy disposed on the surface and in electrical communication with the array of conductive projections, and switching the bias voltage includes providing the bias voltage to the array of conductive projections via the eutectic alloy. Immersing the device includes disposing the device in a flow cell reactor through which the solution flows. A respective conductive projection of the array of conductive projections and a respective catalyst nanoparticle of the plurality of catalyst nanoparticles establish a metal/metal-nitride interface configured to promote the hydrogen production via water splitting. The substrate includes silicon. Each conductive projection of the array of conductive projections includes a III-nitride semiconductor material. Each catalyst nanoparticle of the plurality of catalyst nanoparticles includes a platinum nanocluster. The first and second contacts include a eutectic alloy on the backside of the substrate and the surface of the substrate, respectively. The device further includes a switch to apply a bias voltage to either the first contact or the second contact. The device further includes an oxide passivation layer covering the plurality of catalyst nanoparticles. The oxide passivation layer includes titanium oxide. Each conductive projection of the array of conductive projections has a semiconductor composition. The semiconductor composition of each conductive projection of the array of conductive projections is terminated with nitrogen along surfaces of the conductive projection. Each conductive projection of the array of conductive projections includes a nanowire. Each catalyst nanoparticle of the plurality of catalyst nanoparticles includes platinum. A respective conductive projection of the array of conductive projections and a respective catalyst nanoparticle of the plurality of catalyst nanoparticles establish a metal/metal-nitride interface configured to promote hydrogen production via water splitting. Each catalyst of the plurality of catalysts includes platinum. Each catalyst of the plurality of catalysts includes a rare earth element. The metal-nitride semiconductor material is GaN. The method further includes forming first and second electrical connections to the array of nanowires and the substrate, respectively. Forming the first and second electrical connections to the array of nanowires and the substrate includes disposing a eutectic alloy on the surface of the substrate and a backside of the substrate, respectively. The method further includes passivating the plurality of catalyst nanoparticles and the array of nanowires with an oxide layer. Passivating the plurality of catalyst nanoparticles and the array of nanowires includes depositing titanium oxide via atomic layer deposition. Depositing the plurality of catalyst nanoparticles includes implementing a photo-deposition procedure with platinum. Growing the array of nanowires includes implementing a molecular beam epitaxy (MBE) procedure with N-rich conditions. The eutectic alloy includes GaIn. The method

further includes passivating the backside of the substrate and the electrical connection to the array of nanowires with epoxy.

BRIEF DESCRIPTION OF THE DRAWING FIGURES

[0012] For a more complete understanding of the disclosure, reference should be made to the following detailed description and accompanying drawing figures, in which like reference numerals identify like elements in the figures.

[0013] Figure 1 depicts Pt nanoclusters on GaN nanowires grown on an n^+-p Si wafer in accordance with one example, including (a) a schematic illustration of the fabrication of a Pt/GaN/Si photocathode by epitaxial growth of GaN nanowires (NWs) on a Si p-n wafer and photodeposition of Pt nanoclusters (NCs), (b) a 45º-tilted-view SEM image of the Pt/GaN/Si photocathode, (c) a HAADF-STEM image of Pt/GaN NWs, and STEM-EDS elemental maps of (d) Ga, (e) N, and (f) Pt, and (g) Ga $2p_{3/2}$, (h) N 1s, and (i) Pt 4f XPS spectra for GaN/Si and Pt/GaN/Si electrodes.

[0014] Figure 2 depicts graphical plots of photoelectrochemical seawater hydrogen evolution in accordance with several examples, including (a) LSV curves of Si, Pt/Si, GaN/Si, and Pt/GaN/Si measured with a three-electrode configuration in 0.5 M NaCl solution under AM 1.5G 1 sun illumination or in dark, (b) LSV curves of Pt/GaN/Si in six aqueous solutions including: acidic solutions (pH = 0) of 0.5 M H_2SO_4 and 0.5 M NaCl + 0.5 M H_2SO_4; neutral solutions (pH = 7.4) of 1 M PBS and 0.5 M NaCl + 1 M PBS; and, a weak alkaline solution of 0.5 M NaCl (pH = 9.1) and seawater (pH = 8.2), (c) ABPE of Pt/GaN/Si in seawater, 0.5 M NaCl and 0.5 M NaCl + 1 M PBS, (d) LSV curves of Si, Pt/Si, GaN/Si, and Pt/GaN/Si measured with a two-electrode configuration in 0.5 M NaCl, in which the inset shows the onset potential of each electrode, (e) the amount of H_2 produced and faradaic efficiency of Pt/GaN/Si in 0.5 M NaCl at -3 V versus IrOx, in which the faradaic efficiency is nearly 100%, (f) stability of Pt/GaN/Si in 0.5 M NaCl and seawater at -3 V, in which the photocurrent density retained more than 85% of initial value after 15 h reaction, and in which the inset shows the LSV curves before and after the stability test.

[0015] Figure 3 schematically depicts water dissociation in accordance with one example in which a Pt/GaN interface promotes water splitting, including schematic views of optimized structures and calculated energy changes of (a) water dissociation on Pt(111), (b) proton transfer from surface N–H to a Pt cluster, (c) water dissociation at a Pt-Ga site at the Pt/GaN interface and subsequent H spillover to Pt surface, in which energy changes are shown in

the unit of eV, and white, red, blue, green, and grey spheres represent H, O, N, Ga, and Pt atoms, respectively.

[0016] Figure 4 depicts schematic views of (a) a switchable dual contact electrode (e.g., a PEC/EC switchable electrode) in accordance with one example, in which a front contact is placed on a front side of GaN nanowires (NWs) and a back contact is placed on a back side of an n^+-p Si wafer, and a GaIn eutectic is sandwiched between the contacts (e.g., Cu contacts) and the substrate for Ohmic connection, (b) a front contact for electrochemical HER under dark, and (c) a back contact for photoelectrochemical HER under light, as well as graphical plots of (d) LSV curves of electrode measured with 2-electrode configuration in 0.5 M NaCl solution, (e) onset potential and current density at -2 and -3 V for front and back contacts, in which onset potential is defined as the potential at -10 mA/cm2., and (f) the amount of H_2 produced and faradaic efficiency measured at -2 and 3 V under dark (front contact) and light (back contact) conditions.

[0017] Figure 5 depicts concentrated solar light PEC water splitting in accordance with several examples, including (a) a schematic illustration and (b) photographs of the liquid flow cell for PEC water splitting examples, in which light illuminates the backside of an n^+-p Si wafer and HER takes place on a front side of Pt/GaN nanowires (NWs), as well as graphical plots of LSV curves of a Pt/GaN/Si electrode measured with (c) three-electrode and (d) two-electrode configurations in 0.5 M NaCl under different light intensities, and further graphical plots of (e) a chronoamperometric curve and (f) an amount of H_2 produced and faradaic efficiency measured under light intensities of 1, 3, 6, and 9 suns at -3 V.

[0018] Figure 6 is a schematic view and block diagram of an electrochemical system having a photocathode with an array of nanostructures having a protection arrangement for stable hydrogen evolution via water splitting in accordance with one example.

[0019] Figure 7 is a flow diagram of a method of fabricating of a photocathode having a protection arrangement in accordance with one example.

[0020] Figure 8 is a flow diagram of a method of producing hydrogen from a solution that includes sodium chloride (e.g., seawater) in accordance with one example.

[0021] The embodiments of the disclosed devices, systems, and methods may assume various forms. Specific embodiments are illustrated in the drawing and hereafter described with the understanding that the disclosure is intended to be illustrative. The disclosure is not intended to limit the invention to the specific embodiments described and illustrated herein.

DETAILED DESCRIPTION OF THE DISCLOSURE

[0022] Photoelectrochemical, photocatalytic, and other systems and devices (e.g., photocathodes or photoelectrodes) for hydrogen production and/or other chemical reactions are described. The hydrogen is produced from a solution that includes dissolved sodium chloride (NaCl), such as seawater. Methods of hydrogen production, e.g., using the devices and systems, are also described.

[0023] The devices may include metal/metal-nitride interfaces configured to promote water splitting. The interfaces may be established between conductive projections (e.g., nanowires) composed of, or otherwise including, a metal-nitride semiconductor material, such as GaN, and metal nanoparticles (e.g., nanoclusters) disposed over (e.g., distributed across) the conductive projections. Methods of fabricating the devices (e.g., photoelectrodes or photocatalytic devices) are also described.

[0024] In operation, the disclosed devices are immersed in the seawater or other solution including dissolved NaCl. The pH of the solution may be lowered in preparation for the hydrogen production. However, the solution may be acidic or alkaline. In some cases, the solution is a phosphate-buffered solution.

[0025] The disclosed devices may be illuminated for charge carrier generation and photoelectrochemical operation. For instance, a backside of a substrate of the devices may be illuminated to generate the charge carriers. In some cases, solar radiation may be used to illuminate the devices. The disclosed devices may thus be configured for solar-assisted or solar-driven seawater hydrogen evolution and/or other chemical reactions. The water splitting may be further solar driven in the sense that a bias voltage applied to a contact of the disclosed devices is supported by a photovoltaic device, such as a solar cell.

[0026] In some cases, the disclosed devices include multiple contacts to support both photoelectrochemical (PEC) operation and electrochemical (EC) operation. The PEC operational mode may be used when the device is illuminated (e.g., during daytime), while the EC operational mode may be used when light is not available (e.g., during nighttime). The device may include a switch (e.g., switching electrode) to apply a bias voltage to respective contacts of the device for the PEC and EC operational modes. For instance, a eutectic alloy may be disposed on a substrate surface and a backside opposite the surface for electrical connections to the contacts.

[0027] Although described in connection with photoelectrochemical water splitting, the disclosed devices and systems may be used in other chemical reaction contexts and

applications. For instance, the disclosed devices and systems may be useful in connection with various types of photocatalytic and/or other systems, and/or in connection with other reactions, including, for instance, N_2 reduction, CO_2 reduction to various fuels and other chemicals, NO_3^- reduction, and urea synthesis.

[0028] In some cases, the disclosed devices may include an oxide passivation layer for protection of the catalysts and/or other elements of the disclosed photoelectrodes (e.g., photocathodes), photocatalytic devices, or other devices. The oxide passivation layer may be provided by a thin, conformal layer (e.g., a conformal oxide layer). In some cases, the conformal layer is composed of titanium oxide, but additional or alternative oxides may be used. The conformal layer may have a thickness on the order of the size of each catalyst nanoparticle. The thin nature of the conformal layer is configured such that the layer does not inhibit the transfer of charge carriers, e.g., from the photoelectrode structure(s) to reaction sites along the photoelectrode. The conformal layer is nonetheless still sufficiently thick to cover, and therefore protect, the catalyst arrangement. For instance, protection of the catalyst nanoparticles and/or other surface passivation is thus provided despite the thin nature of the oxide or other conformal layer.

[0029] Alternative or additional surface protection is provided by a nitrogen-based surface of the disclosed photoelectrode. In cases involving an array of nanostructures, each nanostructure may be composed of, or otherwise include, a compound semiconductor that establishes the nitrogen-based surface. For instance, the nanostructures may be composed of, or otherwise include, GaN in an arrangement in which the surface is nitrogen-terminated. Alternatively or additionally, the disclosed photoelectrodes may have one or more surfaces on which a nitrogen or other nitrogen-based layer is disposed.

[0030] In some cases, the disclosed devices may include an array of N-terminated nanowires (e.g., GaN nanowires) grown on Si. The nanowires may effectively protect the underlying Si photocathode against degradation, e.g., for over 3000 hours in acidic electrolytes. Moreover, as described herein, the co-catalysts supported on the GaN nanowires exhibit unique catalytic performance arising from the cocatalyst-GaN interface while remaining stable for enhanced water splitting of seawater.

[0031] Examples of Si photocathodes having Pt nanoclusters (NCs) on GaN nanowires are described below. The efficiency and stability of the Si photocathodes as applied to seawater PEC hydrogen evolution are addressed. The GaN nanowires are loaded with catalytic Pt nanoclusters and grown on Si photocathodes. The nanowire-nanocluster arrangement catalyzes water splitting while protecting the Si wafers from corrosion. Further, DFT

calculations show that Pt-Ga sites at the Pt/GaN interface promote the adsorption and activation of water molecules. The dissociated H^* atoms spill over to neighboring Pt nanoclusters, which facilitate H_2 evolution. As a result, the example Pt/GaN/Si photocathodes achieved a current density of -10 mA/cm^2 at 0.15 and 0.39 V *vs.* RHE (V_{RHE}) and high applied bias photon-to-current efficiency (ABPE) of 1.6% and 7.9% in seawater (pH = 9.1) and phosphate-buffered seawater (pH = 7.4), respectively. The example photocathodes exhibited a current density of -10 mA/cm^2 at a small potential of -1.45 V *vs* IrO_x with a 2-electrode configuration, and operated steadily over a period of over 120 hours, indicating superior performance compared to photocathodes without GaN nanowires. Under concentrated solar light (9 suns), a high current density of about -169 mA/cm^2 continuously generated high-purity hydrogen (H_2).

[0032] Although described herein in connection with electrodes having GaN-based nanowire arrays for water splitting, the disclosed devices and systems are not limited to GaN-based nanowire arrays. A wide variety of other types of nanostructures and other conductive projections may be used. In some cases, the electrodes of the disclosed systems do not include an array of nanowires, and instead include other shaped projections. Thus, the nature, construction, configuration, characteristics, shape, and other aspects of the electrodes may vary.

[0033] Although described herein in connection with electrodes having platinum nanocluster catalysts for water splitting, the disclosed devices and methods are not limited to platinum nanoclusters. Other materials and other nanoparticle structures may be used. Thus, the nature, construction, configuration, characteristics, shape, and other aspects of the nanoparticle catalysts may vary.

[0034] Figure 1 depicts a photocathode having a PtGaN/Si microstructure in accordance with one example. In this case, GaN nanowires were grown on an n^+-p Si (100) substrate via plasma-assisted molecular-beam epitaxy (MBE) under nitrogen rich conditions (Figure 1, part a). Pt nanoclusters were deposited to coat the surfaces of the GaN nanowires. In this case, the nanoclusters were applied by photochemical deposition, for which further details are provided below. A scanning electron microscopy (SEM) image shows that the GaN nanowires were vertically aligned on the planar n^+-p Si substrate with a length of about 400 nm and a diameter of about 50 nm (Figure 1, part b). The Pt nanoclusters are not clearly seen in the SEM image due to their small size.

[0035] The microstructures of the GaN nanowires and Pt nanoclusters were analyzed by scanning transmission electron microscopy (STEM). In the high angular annular dark field

(HAADF)-STEM image (Figure 1, part c), Z-contrasts from the locally segregated Pt nanoclusters were found on the GaN nanowires because of the large difference in atomic number between Pt (78) and Ga (31). The atomic distribution was elucidated by STEM-EDS elemental maps (Figure 1, parts d-f). Ga, N, and Pt elements were found to be uniformly distributed over the entire surface of GaN nanowires. X-ray diffraction (XRD) patterns of the Pt/GaN/Si microstructure showed GaN (002) and (004) peaks. However, the XRD peaks of crystallite Pt nanoclusters were not detected due to the small size of the crystallite Pt nanoclusters.

[0036] X-ray photoelectron spectroscopy (XPS) was performed to analyze the surface bonding states of GaN/Si and Pt/GaN/Si microstructures. Ga $2p_{3/2}$ XPS spectra were deconvoluted with a major peak of Ga-N bond (1118.4 eV) and a minor peak of Ga-O or Ga-OH bond (1119.6 eV) (Figure 1, part g). In the N 1s XPS spectra, the photoelectrons originating from N-Ga (398.2 eV) and N-H (399.7 V) were detected together with Ga LMM Auger electrons (Figure 1, part h). The intensity and energy position of bonding states remained almost identical in the Ga $2p_{3/2}$ and N *1s* spectra after deposition of Pt nanoclusters, indicating that the N-rich GaN nanowires were stable during the photo-deposition against photochemical reaction in the aqueous solution. The Pt *4f* XPS spectrum, with two doublets of $4f_{5/2}$ and $4f_{7/2}$, was analyzed for Pt^0 (71.3 and 74.5 eV) and Pt^{2+} (72.3 and 75.6 eV) bonds (Figure 1, part i). Pt nanoclusters included mainly metallic Pt bonds with a small portion of Pt^{2+} bonds likely due to surface absorbed oxygen or a Pt-N bond at the interface between Pt and GaN. For comparison, a control electrode of Pt/Si was prepared through photo-deposition of Pt nanoclusters on planar n^+-p Si and showed a Pt *4f* XPS spectrum with similar bonding states.

[0037] The performance of the device examples in photoelectrochemical seawater splitting was then evaluated. The PEC hydrogen evolution reaction was performed by a simulated AM1.5G solar spectrum incident on the Pt-decorated GaN nanowire array at an angle normal to the planar n^+-p Si wafer. The conduction band edge of GaN is positioned above the redox potential of the hydrogen evolution reaction, indicating appropriate energy band structure for electron transfer. An electrical bias was applied to the backside of the Si wafer. Linear sweep voltammetry (LSV) curves of Si, Pt/Si, GaN/Si, and Pt/GaN/Si microstructures were measured in 0.5 M NaCl (pH = 9.1) with a three-electrode configuration under 1-sun (100 mW/cm^2) illumination (Figure 2, part a). The potentials at -10 mA/cm^2 (η_{10}) were -1.42, -1.41, -0.83, and 0.16 V_{RHE} for the Si, Pt/Si, GaN/Si, and Pt/GaN/Si microstructures, respectively. Both GaN nanowires and Pt nanoclusters improved the activity of the PEC

hydrogen evolution reaction. The synergistic interaction between GaN nanowires and Pt nanoclusters played a useful role in achieving a high catalytic activity of the Pt/GaN/Si microstructure. The saturated current densities of the GaN/Si and Pt/GaN/Si microstructures (about 35 mA/cm^2) were larger than those without GaN nanowires (about 30 mA/cm^2) because the GaN nanowires provide an enlarged surface area, and reduce the Fresnel reflection loss. The Pt/GaN/Si microstructure exhibited negligible current density in darkness due to the absence of the photogenerated charge carriers.

[0038] The example Pt/GaN/Si microstructure was evaluated in six different solutions (Figure 2, part b) to investigate the effect of pH and the effect of the ions in the solution. The Pt/GaN/Si microstructure exhibited high PEC hydrogen evolution reaction activity ($\eta_{10} > 0.3$ V_{RHE}) in 0.5 M H_2SO_4 solutions (pH = 0) and 1 M phosphate-buffered solutions (PBS) (pH = 7.4), even with dissolved NaCl. Despite having slightly worse hydrogen evolution reaction performance than acidic and neutral solutions due to the lack of H^+ ions near the electrode surface, the hydrogen evolution reaction in 0.5 M NaCl (pH = 9.1) and seawater (pH = 8.2) was still demonstrated at applied potentials > 0 V_{RHE}. As a result, high ABPE of 7.9%, 1.6%, and 1.7% were achieved in 0.5 M NaCl + 1 M PBS, 0.5 M NaCl, and seawater, respectively (Figure 2, part c). On the other hand, the PEC hydrogen evolution reaction performance of the Pt/Si microstructure significantly degraded in 0.5 M NaCl and 0.5 M NaCl + 1 M PBS. These findings revealed that the Pt/Si microstructure exhibited poor catalytic activity due to the sluggish kinetics of water dissociation in the neutral electrolyte. Moreover, the LSV curves of the Pt/GaN/Si microstructure were identical in solutions with different NaCl concentrations, confirming the feasibility for seawater hydrogen evolution.

[0039] To test for practical photoelectrolysis, LSV curves were measured in 0.5 M NaCl solution with a two-electrode configuration *vs.* iridium oxide (IrO_x) counter electrode (Figure 2, part d). η_{10} was -3.41, -3.47, -2.85, and -1.88 V for the Si, Pt/Si, GaN/Si, and Pt/GaN/Si microstructures, respectively. η_{10} was improved to -1.33 and -1.45 V when measured in acidic (0.5 M NaCl + 0.5 M H_2SO_4) and phosphate-buffered (0.5 M NaCl + 1 M PBS) seawater, respectively. To the best of the applicant's knowledge, -1.45 V is the best η_{10} among PEC and EC HER electrodes in neutral-pH seawater.

[0040] The faradaic efficiency of H_2 and O_2 produced from the Pt/GaN/Si microstructure with a two-electrode configuration was further evaluated in 0.5 M NaCl and seawater. At -2 V *vs* IrO_x, the H_2 production rate was 275 $\mu mol/cm^2/h$, and the O_2 production rate was 128 $\mu mol/cm^2/h$ in 0.5 M NaCl. The H_2/O_2 ratio (2.15) nearly approaches the theoretical value (2) for water splitting. When a larger potential (-3 V *vs* IrO_x) was applied to the photocathode,

the H_2 and O_2 production rates were 600 and 216 μmol/cm^2/h in 0.5 M NaCl (Figure 2, part e), and 575 and 159 μmol/cm^2/h in seawater, respectively. Regardless of electrolyte and applied potential, faradaic efficiency of H_2 was almost 100%, confirming high efficiency of electron utilization. Meanwhile faradaic efficiency of O_2 was decreased from 93% to 61-75% by increasing the potential from -2 to -3 V *vs* IrO_x likely due to Cl^- oxidation reactions.

[0041] The example devices exhibited stability with little degradation in chronoamperometric (CA) and LSV curves after reaction for 15 hours in 0.5 M NaCl and seawater (Figure 2, part f). There was no noticeable change in morphology and microstructure of the Pt/GaN/Si microstructure. Compared with the rapid degradation of the Pt/Si microstructure, clearly, the physical and chemical stability of Si photoelectrodes with GaN nanowires and Pt nanoclusters is greatly improved. Furthermore, the performance of the Pt/GaN/Si microstructure is capable of being fully recovered after the re-deposition of Pt nanoclusters, indicating that removal of Pt nanoclusters in seawater constitutes the reason for the degradation. Although the catalytic activity was slightly decreased with a thin TiO_2 layer (2 nm) on the Pt/GaN/Si microstructure, the Pt nanoclusters are stabilized on the GaN nanowires, leading to long-term stability, e.g., for over 120 hours in pH neutral seawater.

[0042] Theoretical modeling was implemented to explore the mechanistic role played by the Pt/GaN binary system via periodic density function theory (DFT) calculations. While Pt and other catalysts are capable of proton reduction, Pt is not good at water reduction under neutral or alkaline solution because the water dissociation is the bottleneck for efficient hydrogen evolution under those conditions. Therefore, the modeling focused on the water dissociation step on Pt(111) and Pt/GaN interface to provide mechanistic understanding of the good performance of the Pt/GaN binary system.

[0043] The dissociation of water on the Pt(111) surface was first analyzed. The H–OH bond cleavage is highly endothermic on Pt(111), with an energy change of 0.72 eV (Figure 3, part a). This is consistent with the experimental fact that Pt is not an effective catalyst for H_2 production in neutral or alkaline solutions. Water is known to dissociate on the GaN m-plane due to the high polarity of the surface. When a water molecule approaches the GaN $(10\bar{1}0)$ surface, it spontaneously dissociates to H^+ and OH^-. The OH^- coordinates to Ga and the H^+ binds to N. However, the transfer of a proton from the surface N–H group to the Pt cluster was found to be highly endothermic by 1.38 eV (Figure 3, part b), probably due to the high pKa of NH groups. At the same time, water dissociation at a Pt-Ga site of the Pt/GaN interface was found to be quite favorable, with an energy change of -0.67 eV (Figure 3, part c).

[0044] A gallium oxynitride (GaON) layer may be formed on the surface of GaN under the condition of photoelectrochemical water splitting. Further details regarding the GaON layer are set forth in International Patent Publication No. WO 2022/187133 ("Crystallographic- and Oxynitride-Based Surface Stabilization"), the entire disclosure of which is hereby incorporated by reference.

[0045] In order to investigate the dependence of water dissociation energetics on the GaN and GaON surface, water dissociation at the Pt-Ga site of the Pt/GaON interface was studied. The energy change of water dissociation is similar to that at the Pt/GaN interface. Compared to water dissociation on Pt(111), the dissociation of water at a Pt-Ga site benefits from the asymmetric atomic environment that facilitates the heterolytic cleavage of the H–OH bond to form Pt–H and Ga–OH. The *H spontaneously spills over to neighboring Pt atoms, with a ΔE of -0.15 eV. So, the overall energy change due to water splitting at the Pt/GaN interface is -0.81 eV. Effective water dissociation at the Pt-Ga site is likely responsible for the high activity of seawater splitting on Pt/GaN/Si in neutral pH or weakly alkaline solutions. Interestingly, the difference in water dissociation energy ΔE when comparing Pt(111) and Pt-Ga site is 1.53 eV, similar to the difference in overpotential ($\Delta\eta_{10}$ = 1.58 V) between the Pt/Si and Pt/GaN/Si electrodes, indicating the utility of the Pt-Ga sites at the Pt/GaN interface for achieving efficient water splitting.

[0046] Operation of the example devices in concentrated solar light PEC seawater splitting is now described. Concentrated solar light enhances the number of photogenerated electrons in the semiconductor and increases the photocurrent for the PEC hydrogen evolution reaction. However, the reaction kinetics under concentrated solar light with vigorous H_2 evolution may be limited by mass transport and shielding of active sites by gaseous bubbles. A flow cell can simultaneously solve these two issues by fast delivery of the reagent and the physical detachment of gas bubbles from the electrode surface. Hence, a liquid flow cell reactor may be used for the concentrated solar light PEC seawater splitting to demonstrate high photocurrent density (Figure 4, part a). Light was incident on the backside of the n^+-p Si wafer while the PEC hydrogen evolution reaction occurred on the front side in the reactor (Figure 4, part b). In this example, 0.5 M NaCl solution continuously flowed at a rate of 20 ml/min during the measurement. The Pt/GaN/Si microstructure achieved an η_{10} of about 0.2 V_{RHE} and saturated current density of about -19 mA/cm^2 under 1 sun light (Figure 4, part c). As the light was intensified to 3, 6, and 9 suns, the saturated current density increased to about -58, about -118, and about -163 mA/cm^2, respectively. In the two-electrode configuration, the Pt/GaN/Si microstructure also showed a gradual

increase in the photocurrent density, reaching a high value of about -165 mA/cm^2 at -3.2 V under 9 suns light illumination (Figure 4, part d). The linear correlation between the light intensity and the saturation current density indicates that the light intensity and the number of photogenerated electrons in the photoelectrode are the limiting factors for the PEC hydrogen evolution reaction in the flow cell.

[0047] CA measurements were evaluated for 4 hours under 1, 3, 6, and 9 suns at -3 V *vs* IrO_x (Figure 4, part e). The current densities for each period of reactions (-20, -60, -121, and -169 mA/cm^2, respectively) were stable in 0.5 M NaCl. This is a record high photocurrent density for the PEC hydrogen evolution reaction among photocathodes in aqueous electrolytes.

[0048] The amount of H_2 product and faradaic efficiency were monitored for 4 hours at -3 V under different light intensities (Figure 4, part f). The production rate gradually increased from 359 to 3351 μmol/cm^2/h as the incident illumination was intensified from 1 to 9 suns. The faradaic efficiency was nearly 100% regardless of the light intensity, confirming that all photocurrents participated in the hydrogen evolution reaction. Moreover, two individual photocathodes were tested for 4 hours at -3 V under 9 suns in 0.5 M NaCl. Both samples showed average photocurrent densities of 166 and 157 mA/cm^2 without degradation, indicating remarkable stability even with vigorous gas bubbling. Furthermore, the concentrated solar light experiment was conducted in phosphate-buffered solution (0.5 M NaCl + 1 M PBS) and exhibited high photocurrent density (greater than 160 mA/cm^2), near-unity faradaic efficiency (about 100%), and positive shift of potential by about 0.1 V. Therefore, the Pt/GaN/Si microstructure of the example device realizes a highly efficient, selective, and stable photocathode for seawater splitting.

[0049] In some cases, the disclosed devices may be configured for both PEC (light) and electrochemical (dark) operation. The device may include a switch or switchable electrode to support both operational modes as described below.

[0050] The GaN nanowires may be degenerately doped n-type and are highly electrically conductive with the loading of large densities of Pt nanoclusters. Hence, an electrical contact at the front side of GaN nanowires/Si wafer may establish a cathode for the electrochemical hydrogen evolution reaction. Therefore, the Pt/GaN/Si microstructure may work under either light or dark conditions by switching the contact positions (Figure 5, part a). During the electrochemical hydrogen evolution reaction in the dark, the electrical bias injects electrons into the GaN nanowires, which drift to Pt nanoclusters leading to H_2 evolution (Figure 5, part b). In contrast, during the PEC hydrogen evolution reaction with light, the n^+-p Si substrate

with a narrow bandgap (about 1.1 eV) generates electron-hole pairs by solar irradiation (Figure 5, part c). The photogenerated electrons in the conduction band migrate toward the *n*-type GaN nanowires and Pt nanoclusters for the hydrogen evolution reaction, whereas holes move to the back contact and counter electrode and engage in the anodic reaction.

[0051] The performance of the switchable electrode was assessed with an example device immersed in a 0.5 M NaCl solution (Figure 5, part d). There was no photoresponse when the front contact was in use, *i.e.,* when operating in the electrochemical mode; LSV curves under dark and light conditions overlapped. On the contrary, when the back contact was used (*i.e.,* PEC mode), there was no photocurrent in the dark, whereas η_{10} was 0.11 V_{RHE} in a three-electrode configuration and -1.83 V in a two-electrode configuration under 1 sun light irradiation, respectively. The built-in-potential of the Si p-n junction can shift positively the onset potential by about 0.4 V compared to the electrochemical reaction and realize a relatively high current density (-17.5 mA/cm^2) at a low operating voltage (-2 V) (Figure 5, part e). Yet, the photocurrent density was saturated to about 35 mA/cm^2 limited by minority carrier diffusion in reverse bias as well as the number of photogenerated charge carriers. As the electrochemical hydrogen evolution reaction was performed using the front contact in the dark, there was a higher yield of H_2 (-58 mA/cm^2) at -3 V. The high quality of degenerately doped n-type GaN nanowires, evidenced by the enhancement of saturation photocurrent density of the Pt/GaN/Si assembly in comparison with a Pt/Si microstructure, allows for the usage of majority carriers for the hydrogen evolution reaction due to factors such as the absence of Fermi level pinning and efficient electron transport to Pt at the non-polar sidewalls. Furthermore, the productivity and faradaic efficiency of the Pt/GaN/Si microstructure were measured at -2 and -3 V under dark and light conditions (Figure 5, part f). At -2 V, the production rate was 100 and 276 μmol/cm^2/h under dark and light, respectively, showing that the PEC hydrogen evolution reaction is more favored than the electrochemical hydrogen evolution reaction under light illumination. On the other hand, at the more negative potential of -3 V, the production rate of electrochemical HER (1125 μmol/cm^2/h) was about 2 times higher than the PEC hydrogen evolution reaction (562 μmol/cm^2/h). Remarkably, the faradaic efficiency was almost 100% for all conditions. Therefore, the Pt/GaN/Si assembly is capable of operation as a photocathode during the day and as an electrocatalyst at night for continuous generation of clean hydrogen.

[0052] The above-described examples demonstrate that Pt nanoclusters bound to GaN nanowires are highly active for the PEC hydrogen evolution reaction in acidic, neutral, and weak alkaline solutions of seawater. DFT calculations further confirmed that the Pt-Ga sites

at the Pt/GaN interface promote the dissociation of water and facilitate H_2 evolution. The Pt/GaN on Si electrodes is thus a synergetic binary system for achieving highly efficient catalytic hydrogen evolution over a wide range of pH. The Pt/GaN/Si microstructures exhibited superior η_{10} = 0.15 and 0.39 V_{RHE} with a high ABPE = 1.7%, 1.6% and 7.9% in seawater (pH = 8.2), 0.5 M NaCl (pH = 9.1), and phosphate-buffered seawater (pH = 7.4), respectively. In the two-electrode configuration, the photocathode operated over 120 hours and generated a record-high photocurrent density of about -169 mA/cm^2 under concentrated solar light (9 suns). The measured efficiency and stability are among the highest values ever reported for the PEC hydrogen evolution reaction in seawater. Importantly, the Pt/GaN/Si microstructures are capable of uniquely operating in both light (PEC) and dark (electrochemical) conditions. The reported findings show that the Pt/GaN/Si assembly promotes catalytic reactions and can be used as an energy-saving electrode, with superior performance when compared to conventional photoelectrolytic systems.

[0053] Figure 6 depicts a system 100 for hydrogen evolution via water splitting in accordance with one example. The system 100 may also be configured for other reactions. The system 100 may be configured as an electrochemical system. In this example, the electrochemical system 100 is a photoelectrochemical (PEC) system in which solar and/or other radiation is used to facilitate the hydrogen evolution and water splitting. The water splitting may be assisted or unassisted. For instance, unassisted water splitting (e.g., solar-only-driven operation) may be implemented in connection with InGaN nanowires having a tunnel junction. The manner in which the PEC system 100 is illuminated may vary. The wavelength and other characteristics of the radiation may vary accordingly.

[0054] The electrochemical system 100 includes one or more electrochemical cells 102. A single electrochemical cell 102 is shown for ease in illustration and description. The electrochemical cell 102 and other components of the electrochemical system 100 are depicted schematically in Figure 6 also for ease in illustration. The cell 102 contains an electrolyte solution 104. The solution 104 includes dissolved NaCl, and may be acidic, neutral or alkaline, as described herein. In some cases, a CO_2 and/or other source is applied. In some cases, the electrolyte solution is saturated with CO_2. Additional or alternative electrolytes may be used, as described below. Further details regarding examples of the electrochemical system 100 are provided below.

[0055] In the example of Figure 6, the electrochemical cell 102 has a three-electrode configuration. The electrochemical cell 102 includes a working electrode 108, a counter electrode 110, and a reference electrode 112, each of which is immersed in the electrolyte

104. The counter electrode 110 may be or include a metal wire, such as a platinum wire. The reference electrode 112 may be configured as a reversible hydrogen electrode (RHE) (e.g., Ag/AgCl filled with 3 M KCl). The positioning of the reference electrode 112 may vary from the example shown. For example, the reference electrode 112 may be adjacent to the counter electrode 110 in other cases. The configuration of the counter and reference electrodes 110, 112 may vary. For example, the counter electrode 110 may be configured as, or otherwise include, a photoanode at which water oxidation ($4H_2O \Leftrightarrow 2O_2 + 8e^- + 8H^+$) occurs. In some cases, the counter electrode 110 is configured as, or otherwise includes, an IrOx electrode. The configuration of the electrochemical cell may vary. For instance, in other cases, a two-electrode or other configuration may be used.

[0056] The hydrogen evolution occurs at the working electrode 108 as follows:

Hydrogen evolution: $2H_2O + 2e^- \Leftrightarrow H_2 + 2OH^-$

To that end, electrons may flow from the counter electrode 110 through a circuit path external to the electrochemical cell 102 to reach the working electrode 108. The working and counter electrodes 108, 110 may thus be considered a cathode and an anode, respectively. As described above, the dissociation of water may also occur at the working electrode 108.

[0057] In the example of Figure 6, the working and counter electrodes are separated from one another by a membrane 114, e.g., a proton-exchange membrane. The construction, composition, configuration and other characteristics of the membrane 114 may vary.

[0058] In the example of Figure 6, the circuit path includes a voltage source 116 of the electrochemical system 100. The voltage source 116 is configured to apply a bias voltage between the working and counter electrodes 108, 110. The bias voltage may be used to establish a ratio of CO_2 reduction to hydrogen (H_2) evolution at the working electrode, and/or another reaction ratio(s). The circuit path may include additional or alternative components. For example, the circuit path may include a potentiometer in some cases. In other cases, no bias voltage is applied - e.g., in unassisted systems.

[0059] In this example, the working electrode 108 is configured as a photocathode. Light 118, such as solar radiation, may be incident upon the working electrode 108 as shown. The electrochemical cell 102 may thus be considered and configured as a photoelectrochemical cell. In such cases, illumination of the working electrode 108 may cause charge carriers to be generated in the working electrode 108. Electrons that reach the surface of the working electrode 108 may then be used in the hydrogen evolution. The photogenerated electrons may augment electrons provided via the current path.

Alternatively or additionally, the electrons provided via the current path may recombine with the photogenerated holes at a backside or other contact. Further details regarding examples of photocathodes are provided below.

[0060] The working electrode 108 includes a substrate 120. The substrate 120 of the working electrode 108 may constitute a part of an architecture, a scaffolding, or other support structure, of the working electrode 108. The substrate 120 may be uniform or composite. For example, the substrate 120 may include any number of layers or other components. The substrate 120 thus may or may not be monolithic. The shape of the substrate 120 may also vary. For instance, the substrate 120 may or may not be planar or flat.

[0061] In the example of Figure 6, the substrate 120 is doped and otherwise configured to present a junction. The substrate 120 of the working electrode 108 may thus be active (functional) in connection with the photogeneration of charge carriers. Alternatively or additionally, the substrate 120 is passive (e.g., structural). The substrate 120 may be configured and act as a support structure for a catalyst arrangement of the working electrode 108, as described below. Alternatively or additionally, the substrate 120 may be composed of, or otherwise include, a material suitable for the growth or other deposition of the catalyst arrangement of the working electrode 108.

[0062] In active or functional cases, the substrate 120 may include a light absorbing material. The light absorbing material is configured to generate charge carriers upon solar or other illumination. The light absorbing material has a bandgap such that incident light generates charge carriers (electron-hole pairs) within the substrate. Some or all of the substrate 120 may be configured for photogeneration of electron-hole pairs. To that end, the substrate 120 may include a semiconductor material. In some cases, the substrate 120 is composed of, or otherwise includes, silicon. For instance, the substrate 120 may be provided as a silicon wafer.

[0063] The silicon may be doped. In the example of Figure 6, the substrate 120 includes a heavily n-type doped layer 122, a moderately or lightly p-type doped layer 123, and a heavily p-type doped layer 124. The arrangement of the layers 122-124 establishes a junction within the substrate 120. The doping arrangement may vary. For example, one or more components of the substrate 120 may be non-doped (intrinsic), or effectively non-doped. The substrate 120 may include alternative or additional layers, including, for instance, support or other structural layers. In other cases, the substrate 120 is not light absorbing.

[0064] The substrate 120 of the working electrode 108 establishes a surface at which a catalyst arrangement is provided. In some cases, catalyst support structures, or scaffolding, of the electrode 108 are provided as described below. As described below, the catalyst support structures may include an array of conductive projections extending outward from a surface of the substrate 120. In other cases, the catalyst arrangement does not include conductive projections. For instance, the catalyst arrangement may include one or more planar structures, such as one or more layers supported by the substrate 120.

[0065] In the example of Figure 6, the working electrode 100 includes an array of nanostructures 126 (or other conductive projections) supported by the substrate 120. Each nanostructure 126 is configured to extract the charge carriers (e.g., electrons) from the substrate 120. The extraction brings the electrons to external sites along the nanostructures 126 for use in the hydrogen evolution.

[0066] In some cases, each nanostructure 126 is configured as a nanowire. Each nanostructure 126 may have a semiconductor composition. In some cases, the semiconductor composition includes a semiconductor core. For instance, the core may be composed of, or otherwise includes, a Group III-V nitride semiconductor material, such as gallium nitride (GaN). Additional or alternative semiconductor materials may be used, including, for instance, indium gallium nitride (InGaN) and/or other III-nitride semiconductor materials.

[0067] The core of each nanowire or other nanostructure 126 may be or include a columnar, post-shaped, or other elongated structure that extends outward (e.g., upward) from the plane of the substrate 120. The semiconductor nanowires or other nanostructures 126 may be grown or formed as described in U.S. Patent No. 8,563,395, the entire disclosure of which is hereby incorporated by reference. The nanostructures 126 may be referred to herein as nanowires with the understanding that the dimensions, size, shape, composition, and other characteristics of the nanostructures 126 or other conductive projections may vary.

[0068] The semiconductor composition of each nanostructure 126 may or may not be configured to facilitate the reaction(s) supported by the electrochemical system 100. The semiconductor composition may be configured for photo-generation of charge carriers, as described below. Alternatively or additionally, the semiconductor composition may be configured to act as a catalyst for the reaction(s). The semiconductor composition may provide other functions, including, for instance, protection of the substrate 120 as described above in connection with GaN examples. Additional or alternative semiconductor materials

may be used, including, for instance, indium nitride, aluminum nitride, boron nitride, aluminum oxide, silicon, and/or their alloys.

[0069] The semiconductor composition of each nanostructure 126 may be configured to provide surface passivation and/or other protection of the photoelectrode 108. For instance, in some cases, the semiconductor composition is terminated with nitrogen along surfaces of the nanostructure 126. The nitrogen termination or other nitrogen-based aspect of the nanostructures 126 may protect the nanostructures 126 and/or other components of the electrode 108 (e.g., the substrate 120) during operation from, e.g., corrosion. Alternative or additional nitrogen-based protection schemes may be used in other cases. For instance, a layer including nitrogen may be deposited or otherwise disposed along the surface of each nanostructure 126 and/or other element of the electrode 108.

[0070] The nanostructures 126 may facilitate the hydrogen evolution and/or another chemical reaction in one or more ways. For instance, each nanostructure 126 may be configured to extract the charge carriers (e.g., electrons) generated in the substrate 120. The extraction brings the electrons to external sites along the nanostructures 126 for use in the hydrogen evolution and/or other chemical reaction. The composition of the nanostructures 122 may also form an interface well-suited for hydrogen evolution and/or another chemical reaction, as explained herein.

[0071] Each nanostructure 126 may be or include a columnar, post-shaped, or other elongated structure that extends outward (e.g., upward) from the plane of the substrate 120. The dimensions, size, shape, composition, and other characteristics of the nanostructures 126 may vary. For instance, each nanostructure 126 may or may not be elongated like a nanowire. Thus, other types of nanostructures from the substrate 120, such as various shaped nanocrystals, may be used.

[0072] In some cases, the nanostructures 126 may be configured to generate electron-hole pairs upon illumination. For instance, the nanostructures 122 may be configured to absorb light at frequencies different than other light absorbing components of the electrode 108. For example, one light absorbing component, such as the substrate 120, may be configured for absorption in the visible or infrared wavelength ranges, while another component may be configured to absorb light at ultraviolet wavelengths. In other cases, the nanostructures 126 are the only light absorbing component of the electrode 108. In still other cases, the substrate 120 is the only light absorbing component of the electrode 108.

[0073] In some cases, each nanowire 126 may include a layered or segmented arrangement of semiconductor materials. For instance, in Group III-nitride examples, the layers or segments of the arrangement may have differing Group III (e.g., indium and gallium) compositions. One or more layers or segments in the arrangement may be configured for absorption of a respective range of wavelengths. Each nanowire 126 may include one or more segments having a compound semiconductor composition (e.g., InGaN) configured for photogeneration of charge carriers. Other layers or segments may be directed to establishing a tunnel junction. Each nanowire 126 may include segments having a compound semiconductor composition (e.g., InGaN) configured to establish a tunnel junction. Each nanowire 126 may also include additional or alternative segments, including, for instance, a segment between the tunnel junction and the substrate 120.

[0074] In other cases, the layered arrangement of semiconductor materials is also used to establish a multi-band structure, such as a quadruple band structure. Each layer or segment of the arrangement may have a different semiconductor composition to establish a different bandgap. The different bandgaps may be useful in connection with absorbing light of differing wavelengths.

[0075] Other layered arrangements may be used. For example, further details regarding the formation and configuration of multi-band structures, including, for instance, triple-band structures, are provided in U.S. Patent No. 9,112,085 ("High efficiency broadband semiconductor nanowire devices") and U.S. Patent No. 9,240,516 ("High efficiency broadband semiconductor nanowire devices"), the entire disclosures of which are incorporated by reference.

[0076] The semiconductor composition of each nanowire 126 may be configured to improve the efficiency of the water splitting in additional ways. For instance, in some cases, the semiconductor composition of each nanowire 126 may include doping to promote charge carrier separation and extraction, as well as facilitate the establishment of a photochemical diode. For example, a dopant concentration of the semiconductor composition may vary laterally.

[0077] In examples involving III-nitride compositions, the dopant may be or include magnesium. Further details regarding the manner in which magnesium doping promotes charge carrier separation and extraction are set forth in U.S. Patent No. 10,576,447 ("Methods and systems relating to photochemical water splitting "), the entire disclosure of which is incorporated by reference. Additional or alternative dopant materials may be used,

including, for instance, silicon, carbon, and beryllium, depending on the semiconductor light absorber of choice.

[0078] The semiconductor device may further include catalyst nanoparticles 136 disposed over the array of nanowires 126. The nanoparticles 136 are distributed across or along the outer surface (e.g., sidewalls) of each nanowire 126. The nanoparticles 136 are configured to facilitate or promote the proton reduction reaction. In some cases, each nanoparticle 136 includes a metal, such as platinum. Other metals or materials may be used, such as rare earth metals. Still other metals may be used, including alloys and/or other metal or metallic combinations. Further details regarding the formation, configuration, functionality, and other characteristics of nanoparticles 136 in conjunction with a nanowire array are set forth in one or more of the above-referenced U.S. patents.

[0079] The distribution of the nanoparticles 136 may be uniform or non-uniform. The nanoparticles may thus be distributed randomly across each nanowire 126. The schematic arrangement of Figure 6 is shown for ease in illustration.

[0080] The electrode 108 also includes an oxide layer 138 covering the catalyst nanoparticles 136 and each nanostructure 126 of the array of nanostructures 126. The oxide layer 138 acts as a passivation and/or other protection layer. For example, the oxide layer 138 may be configured to protect the nanoparticles 136 and/or passivate the surface of the nanostructures 126. In some cases, the oxide layer 138 is composed of, or otherwise includes, titanium oxide. Alternative or additional oxide materials may be used, including, for instance, aluminum oxide, gallium (and/or aluminum) oxide, and/or gallium (and/or aluminum) oxide nitride (or oxynitride).

[0081] The oxide layer 138 may have a thickness on the order of a size of each catalyst nanoparticle 136. For instance, the thickness of the oxide layer 138 may fall within a range of about 1 nm to about 2 nm, but other thicknesses may be used. In these and other cases, the oxide layer 138 conformally covers the catalyst nanoparticles 136 and the array of nanostructures 126. For instance, the oxide layer 138 may conformally cover the sidewalls and other surfaces of the nanostructures 126, as shown in Figure 6. The conformal coverage of the nanostructure surfaces and nanoparticles is depicted schematically for ease in illustration. The thin nature of the oxide layer 138 allows the protection function to be provided without adversely affecting the transfer of charge carriers and other catalysis of the hydrogen evolution and/or other reaction occurring at the electrode 108.

[0082] The nanowires 126 and the nanoparticles 136 are not shown to scale in the schematic depiction of Figure 6. The shape of the nanowires 126 and the nanoparticles may also vary from the example shown.

[0083] The nanoparticle-nanowire catalyst arrangement may be fabricated on a substrate (e.g., a silicon substrate) via nanostructure-engineering. In one example, molecular beam epitaxial (MBE) growth of the nanowires is followed by photo-deposition of the nanoparticles. The photo-deposition of the nanoparticles may be configured to selectively deposit the nanoparticles on the respective sides of the nanowire. Further details regarding example fabrication procedures are provided below, e.g., in connection with Figure 7.

[0084] The disposition of the platinum nanoclusters or other metal catalyst nanoparticles over the array of nanowires or conductive projections establishes metal/metal-nitride interfaces. As described above, the metal/metal-nitride interfaces are configured to promote hydrogen production via water splitting. For instance, in GaN-platinum examples, the Ga-Pt interface promotes the water splitting through dissociation of the water.

[0085] The nanowires 126 facilitate the water splitting in alternative or additional ways. For instance, each nanowire 126 may be configured to extract charge carriers (e.g., electrons) generated in the substrate (e.g., as a result of light absorbed by the substrate 120). The extraction brings the charge carriers to external sites along the nanowires 126 for use in the water splitting or other reactions. For instance, the nanowires 126 may thus form an interface well-suited for evolution of hydrogen, the reduction of CO_2, and/or other reactions.

[0086] The device 100 is configured for operation in a PEC (illuminated) mode and an electrochemical (non-illuminated) mode. The system 100 and/or the working electrode 108 may include a switch 140 to selectively apply a bias voltage. To that end, the working electrode 108 includes multiple contacts. In the example of Figure 6, the working electrode 108 includes a first contact 142 coupled to the backside of the substrate 120 and to which charge carriers photogenerated in the substrate 120 in the photoelectrochemical (PEC) operational mode move. The working electrode 108 includes a second contact 144 coupled to the array of conductive projections 126 to provide charge carriers to the array of conductive projections 126 in the electrochemical (EC) operational mode. The switch 140 may thus provide the bias voltage to either the first contact 142 or the second contact 144. As described herein, one or both of the contacts 142, 144 may include a eutectic alloy on the backside of the substrate and the surface of the substrate, respectively. For instance, a Ga-In eutectic may be sandwiched between a Cu back contact and the n^+-p Si wafer for ohmic

contact. Additional or alternative electrical connections may be used to apply the bias voltage.

[0087] Figure 7 depicts a method 200 of fabricating a photoelectrode or other semiconductor device for photocatalytic water splitting, PEC water splitting, or other photocatalytic reactions, in accordance with one example. The method 200 may be used to manufacture any of the photoelectrodes or other devices described herein or another device. The method 200 may include additional, fewer, or alternative acts. For instance, the method 200 may or may not include one or more acts directed to forming a backside contact of the device (act 230).

[0088] The method 200 may begin with an act 202 in which a substrate is prepared or otherwise provided. The substrate may be or be formed from a silicon wafer. In one example, a 2-inch Si wafer was used, but other (e.g., larger) size wafers may be used. Other semiconductors and substrates may be used.

[0089] The substrate may have a planar or nonplanar surface. In some cases, the act 202 includes an act 204 in which one or more procedures are implemented to clean the substrate. In some cases, a wet or other etch procedure is implemented to define the surface. For example, the etch procedure may be or include a crystallographic etch procedure. In silicon substrate examples, the crystallographic etch procedure may be a KOH etch procedure. In such cases, if the substrate has a <100> orientation, the wet etch procedure establishes that the surface includes a pyramidal textured surface with faces oriented along <111> planes.

[0090] The act 202 may include fewer, additional, or alternative acts. For instance, in the example of Figure 7, the act 202 includes an act 206 in which oxide is removed.

[0091] In one example, a prime-grade polished silicon wafer is etched in 80 °C KOH solution (e.g., 1.8% KOH in weight with 20% isopropanol in volume) for 30 minutes to form the micro-textured surface with Si pyramids. After being neutralized in concentrated hydrochloric acid, the substrate surface is cleaned by acetone and/or methanol, and native oxide is removed by 10% hydrofluoric acid.

[0092] The act 202 may include still further acts. In the example of Figure 7, the act 202 includes an act 208 in which one or more doping procedures (e.g., thermal diffusion procedures) are implemented to form doped regions or layers, and thereby establish a junction, as described herein. Alternatively, the substrate is provided at the outset with a desired dopant concentration profile.

[0093] In one example, a n^+-p Si junction was fabricated through a standard thermal diffusion process using (100) Si wafer. Phosphorus was spin-coated as an n-type dopant on front side of the double-side polished p-type Si (100) wafer, and boron was spin-coated on the other side as a p-type dopant for Ohmic metal contact. The spin-coated wafer was then annealed at 950 ºC under nitrogen atmosphere for 4 hours.

[0094] The method 200 includes an act 210 in which electrode or other device structure(s) is grown or otherwise formed on the substrate. In some cases, a nanowire or other nanostructure array is grown or otherwise formed on the substrate. Each nanowire is formed on the surface of the substrate such that each nanostructure extends outward from the surface of the substrate. Each nanostructure may have a semiconductor composition, as described herein. In one example, GaN nanowires were grown by plasma-assisted molecular beam epitaxy (MBE) under N-rich conditions.

[0095] The nanostructure growth may be achieved in an act 212 in which a molecular beam epitaxy (MBE) procedure is implemented. The substrate may be rotated during the MBE procedure such that each nanostructure is shaped as a cylindrically shaped nanostructure. Each nanostructure may thus have a circular cross-sectional shape, as opposed to a plate-shaped or sheet-shaped nanostructure.

[0096] The MBE procedure may be implemented under nitrogen-rich conditions. The nitrogen-rich conditions may lead to nitrogen-terminated sidewalls and other surfaces, as described herein.

[0097] In some cases, the MBE procedure may be modified to fabricate the arrangement of layers or segments of each nanowire. Various parameters may be adjusted to achieve different composition levels, thereby forming multiple segments. For instance, the substrate temperature may be adjusted in an act 214. Beam equivalent pressures may alternatively or additionally be adjusted. In some cases, a dopant cell temperature is adjusted to control the doping (e.g., Mg doping) of the nanowires.

[0098] In one example, plasma-assisted molecular beam epitaxy was used for growth of GaN nanowires on the n^+ side of the n^+-p Si wafer under nitrogen rich-condition with a N_2 flow rate of 1.0 standard cubic centimeter per minute. The substrate temperature was held at 790 ºC and the growth duration was ~2 h. The forward plasma power was 350 W with Ga flux beam equivalent pressure (BEP) of 5×10^{-8} Torr.

[0099] The method 200 further includes an act 216 in which catalyst nanoparticles are deposited across the array of nanowires. The deposition of the nanoparticles may be

achieved via implementation of a photo-deposition procedure in an act 218. The nanoparticles may be composed of, or otherwise include, a metal, such as platinum, or other metal material (e.g., rare earth metal). A drying act 220 may then be implemented. Further details regarding the photo-deposition procedures are set forth in one or more of the above-referenced U.S. patents.

[00100] In one example, the catalyst nanoparticles were deposited using a photo-deposition procedure in which the GaN/Si microstructure was placed on a Teflon holder in a glass chamber with a quartz window. 10 µl of 0.2 M chloroplatinic acid hydrate (99.9%, Sigma Aldrich), 55 ml of deionized (DI) water, and 11 ml methanol were poured into the glass chamber. The chamber was evacuated using a vacuum pump for 5 minutes. Then, the sample was irradiated using a 300 W xenon lamp for 30 min. Platinum ions from chloroplatinic acid hydrate were reduced and deposited onto GaN nanowires during the light illumination.

[00101] The method 200 may then include an act 222 in which the nanostructures are covered with a passivation or protection layer. The protection layer may be or otherwise include a conformal oxide layer deposited in an act 224. The oxide layer may be composed of, or otherwise include, titanium oxide. The deposition of the act 224 may include implementation of an atomic layer deposition (ALD) procedure, and/or be otherwise configured to control the thickness of the oxide layer as described herein.

[00102] In one example, a 2 nm TiO_2 passivation layer was deposited on the Pt/GaN/Si microstructure via thermal atomic layer deposition (ALD) at 250 C with tetrakis(dimethylamino) titanium as the precursor.

[00103] The method 200 includes an act 226 in which electrical connections are formed. In some cases, the electrical connection are to the substrate backside and the nanowire array, as described herein. In the example of Figure 7, the act 226 includes disposing, in an act 228, a eutectic alloy (e.g., Ga-In) on the backside and surface of the substrate to form the connections. Wires then may be attached to the contacts in an act 230. For instance, the connection to the backside contact may be established by connecting a Cu-wire to the ohmic contact by applying the Ga-In eutectic paste.

[00104] The method 200 may include one or more additional acts directed to forming the contacts of the device. For instance, in some cases, the method 200 includes an act 232 in which one or more contacts or sides of the electrode are passivated (e.g., via application of an epoxy).

[00105] The method 200 may include additional or alternative acts. For instance, the method 200 may include an act in which the photocathode is diced into smaller pieces, e.g., using a diamond pen.

[00106] Figure 8 depicts a method 300 of hydrogen production in accordance with one example. The method 300 may be implemented with the devices and systems described herein, and/or another device or system. The method 300 may be directed to hydrogen evolution in seawater or other solutions including dissolved NaCl.

[00107] The method 300 includes an act 302 in which the solution is provided. In some cases, the pH of the solution is lowered in an act 304. For instance, the solution may be a phosphate buffered solution. The solution may or may not constitute or include seawater. For instance, the solution may be seawater-based or be otherwise derived or formed from seawater.

[00108] In an act 306, a photocathode or other device is immersed in the solution. As described herein, the device includes a substrate having a surface, an array of conductive projections supported by the substrate and extending outward from the surface of the substrate, and a plurality of catalyst nanoparticles disposed over the array of conductive projections. As described above, the device may be disposed in a flow cell reactor in an act 308.

[00109] In some cases, the method 300 includes an act 310 in which the device is illuminated such that charge carriers are photogenerated in the device to support the hydrogen production. The act 310 may include irradiating a backside of the substrate of the device with sunlight in an act 312. Alternative or additional portions of the photocathode or PEC system may be irradiated or otherwise illuminated.

[00110] In act 314, a bias voltage may be applied to the device as described above. The bias voltage may be applied in a PEC operational mode (e.g., while the device is illuminated in the act 310). In some cases, the bias voltage is applied via an electrical connection to the substrate backside of the photocathode in an act 316.

[00111] As described above, the method 300 may also include an act 318 in which the bias voltage is switched for operation in dark (non-illuminated) conditions. Switching the bias voltage supports operation in an electrochemical operational mode. For instance, the electrode switching may provide the bias voltage via an electrical connection to the nanowire array in an act 320.

[00112] The method 300 may include additional or alternative acts. For instance, the method 300 may include another act in which the bias voltage is switched back for electrical connection to the substrate backside for PEC operation.

[00113] Described above are devices and methods of providing seawater electrolysis for production of clean hydrogen fuel. Examples of high performance photocathodes for seawater hydrogen evolution reaction have been realized, including, for instance, n^+-p Si photocathodes with dramatically improved activity and stability for hydrogen evolution reaction in seawater, modified by Pt nanoclusters anchored on GaN nanowires. In those examples, Pt-Ga sites at the Pt/GaN interfaces promote the dissociation of water molecules and spilling H* over to neighboring Pt atoms for efficient H_2 production. Example Pt/GaN/Si photocathodes achieved a current density of -10 mA/cm^2 at 0.15 and 0.39 V *vs.* RHE and high applied bias photon-to-current efficiency of 1.6% and 7.9% in seawater (pH = 9.1) and phosphate-buffered seawater (pH = 7.4), respectively. A photocurrent density of about 169 mA/cm^2 under concentrated solar light (9 suns) was also demonstrated. Moreover, disclosed above are Pt/GaN/Si examples configured for continuously producing H_2 even under dark conditions by simply switching an electrical contact. The disclosed devices and methods therefore provide an efficient, stable, and energy-saving electrode for H_2 generation by seawater splitting.

[00114] The term "about" is used herein in a manner to include deviations from a specified value that would be understood by one of ordinary skill in the art to effectively be the same as the specified value due to, for instance, the absence of appreciable, detectable, or otherwise effective difference in operation, outcome, characteristic, or other aspect of the disclosed methods, devices, and systems.

[00115] The present disclosure has been described with reference to specific examples that are intended to be illustrative only and not to be limiting of the disclosure. Changes, additions and/or deletions may be made to the examples without departing from the spirit and scope of the disclosure.

[00116] The foregoing description is given for clearness of understanding only, and no unnecessary limitations should be understood therefrom.

What is Claimed is:

1. A method of hydrogen production, the method comprising:

providing a solution; and

immersing a device in the solution, the device comprising:

a substrate having a surface;

an array of conductive projections supported by the substrate and extending outward from the surface of the substrate; and

a plurality of catalyst nanoparticles disposed over the array of conductive projections;

wherein the solution comprises dissolved sodium chloride (NaCl).

2. The method of claim 1, wherein the solution comprises seawater.

3. The method of claim 1, wherein the solution is a phosphate-buffered solution.

4. The method of claim 1, wherein providing the solution comprises lowering the pH of the solution.

5. The method of claim 1, further comprising illuminating the device such that charge carriers are photogenerated in the device to support the hydrogen production.

6. The method of claim 5, wherein illuminating the device comprises irradiating a backside of the substrate of the device with sunlight.

7. The method of claim 1, further comprising applying a bias voltage to the device.

8. The method of claim 7, wherein:

the device comprises a contact coupled to a backside of the substrate; and

applying the bias voltage comprises applying the bias voltage to the contact in a photoelectrochemical (PEC) operational mode of the device.

9. The method of claim 7, further comprising, when the device is not illuminated, switching the bias voltage to apply the bias voltage to the array of conductive projections in an electrochemical operational mode of the device.

10. The method of claim 1, wherein:

the device comprises a eutectic alloy disposed on the surface and in electrical communication with the array of conductive projections; and

switching the bias voltage comprises providing the bias voltage to the array of conductive projections via the eutectic alloy.

11. The method of claim 1, wherein immersing the device comprises disposing the device in a flow cell reactor through which the solution flows.

12. The method of claim 1, wherein a respective conductive projection of the array of conductive projections and a respective catalyst nanoparticle of the plurality of catalyst nanoparticles establish a metal/metal-nitride interface configured to promote the hydrogen production via water splitting.

13. The method of claim 1, wherein:

the substrate comprises silicon;

each conductive projection of the array of conductive projections comprises a III-nitride semiconductor material; and

each catalyst nanoparticle of the plurality of catalyst nanoparticles comprises a platinum nanocluster.

14. A device comprising:

a substrate having a surface and a backside opposite the surface;

an array of conductive projections supported by the substrate and extending outward from the surface of the substrate;

a plurality of catalyst nanoparticles disposed over the array of conductive projections;

a first contact coupled to the backside and to which charge carriers photogenerated in the substrate in a photoelectrochemical (PEC) operational mode of the device move; and

a second contact coupled to the array of conductive projections to provide charge carriers to the array of conductive projections in an electrochemical (EC) operational mode of the device.

15. The device of claim 14, wherein the first and second contacts comprise a eutectic alloy on the backside of the substrate and the surface of the substrate, respectively.

16. The device of claim 14, further comprising a switch to apply a bias voltage to either the first contact or the second contact.

17. The device of claim 14, further comprising an oxide passivation layer covering the plurality of catalyst nanoparticles.

18. The device of claim 17, wherein the oxide passivation layer comprises titanium oxide.

19. The device of claim 14, wherein:

each conductive projection of the array of conductive projections has a semiconductor composition; and

the semiconductor composition of each conductive projection of the array of conductive projections is terminated with nitrogen along surfaces of the conductive projection.

20. The device of claim 14, wherein each conductive projection of the array of conductive projections comprises a nanowire.

21. The device of claim 14, wherein each catalyst nanoparticle of the plurality of catalyst nanoparticles comprises platinum.

22. The device of claim 14, wherein a respective conductive projection of the array of conductive projections and a respective catalyst nanoparticle of the plurality of catalyst nanoparticles establish a metal/metal-nitride interface configured to promote hydrogen production via water splitting.

23. A device comprising:

a substrate having a surface;

an array of conductive projections supported by the substrate and extending outward from the surface of the substrate, each conductive projection of the array of conductive projections comprising a metal-nitride semiconductor material; and

a plurality of metal catalysts disposed over the array of conductive projections such that metal/metal-nitride interfaces are established;

wherein the metal/metal-nitride interfaces are configured to promote hydrogen production via water splitting.

24. The device of claim 23, wherein each catalyst of the plurality of catalysts comprises platinum.

25. The device of claim 23, wherein each catalyst of the plurality of catalysts comprises a rare earth element.

26. The device of claim 23, wherein the metal-nitride semiconductor material is GaN.

27. A method of fabricating a hydrogen production device, the method comprising:

providing a substrate having a surface;

growing an array of nanowires on the surface of the substrate such that each nanowire of the array of nanowires extends outward from the surface of the substrate, each conductive projection of the array of conductive projections comprising a metal-nitride semiconductor material; and

depositing a plurality of metal catalyst nanoparticles across the array of nanowires such that metal/metal-nitride interfaces are established, the metal/metal-nitride interfaces being configured to promote hydrogen production via water splitting.

28. The method of claim 27, further comprising forming first and second electrical connections to the array of nanowires and the substrate, respectively.

29. The method of claim 28, wherein forming the first and second electrical connections to the array of nanowires and the substrate comprises disposing a eutectic alloy on the surface of the substrate and a backside of the substrate, respectively.

30. The method of claim 27, further comprising passivating the plurality of catalyst nanoparticles and the array of nanowires with an oxide layer.

31. The method of claim 30, wherein passivating the plurality of catalyst nanoparticles and the array of nanowires comprises depositing titanium oxide via atomic layer deposition.

32. The method of claim 27, wherein depositing the plurality of catalyst nanoparticles comprises implementing a photo-deposition procedure with platinum.

33. The method of claim 27, wherein growing the array of nanowires comprises implementing a molecular beam epitaxy (MBE) procedure with N-rich conditions.

34. The method of claim 27, wherein the eutectic alloy comprises GaIn.

35. The method of claim 27, further comprising passivating the backside of the substrate and the electrical connection to the array of nanowires with epoxy.

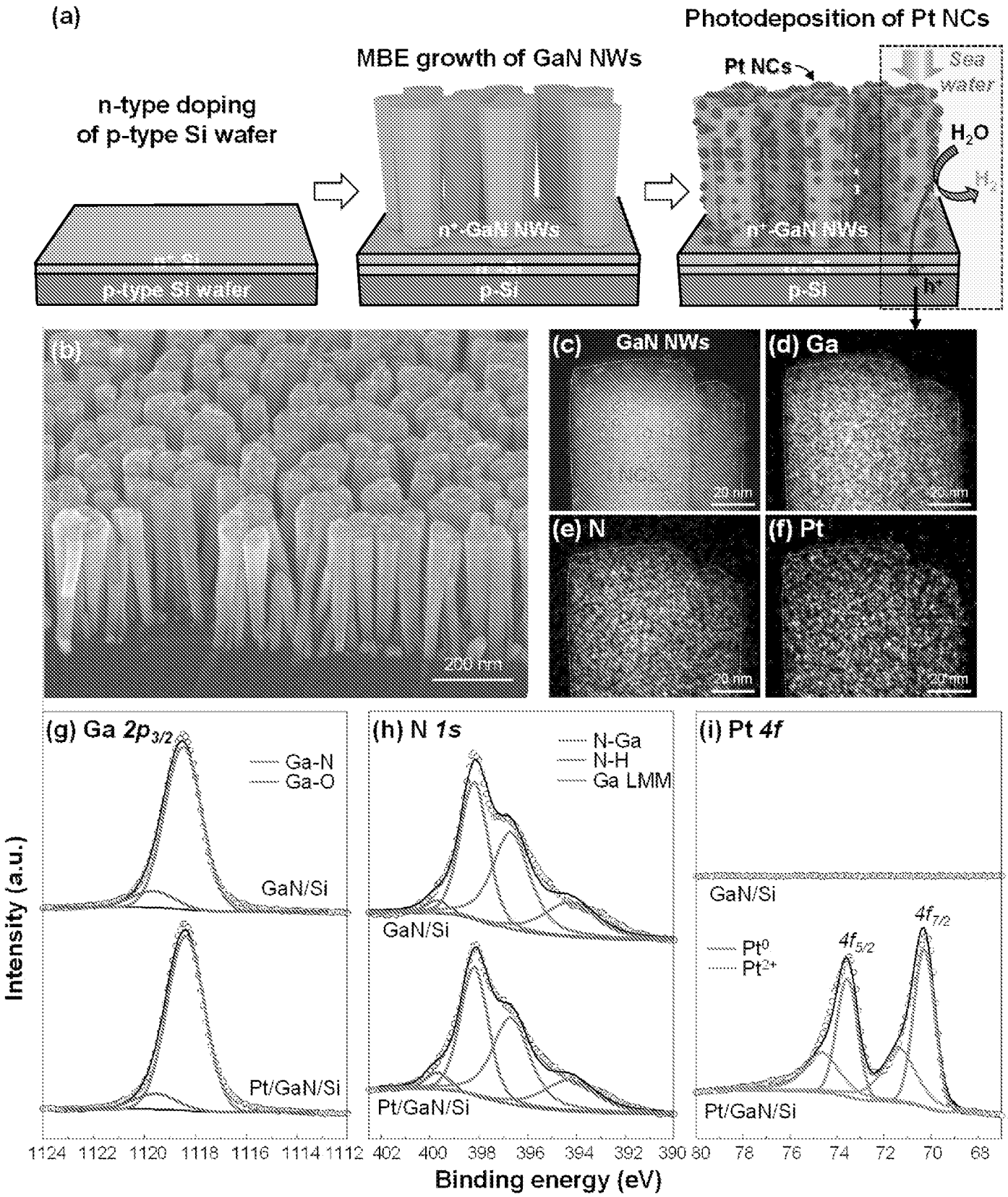
(a)
Photodeposition of Pt NCs
MBE growth of GaN NWs
n-type doping
of p-type Si wafer
Pt NCs
Sea water
H_2O
H_2
n⁺-GaN NWs
p-Si
p-type Si wafer
h⁺
(b)
200 nm
(c) GaN NWs
(d) Ga
(e) N
(f) Pt
20 nm
(g) Ga $2p_{3/2}$
Ga-N
Ga-O
GaN/Si
Pt/GaN/Si
(h) N 1s
N-Ga
N-H
Ga LMM
(i) Pt 4f
$4f_{7/2}$
$4f_{5/2}$
Pt^0
Pt^{2+}
Intensity (a.u.)
Binding energy (eV)
1124 1122 1120 1118 1116 1114 1112
402 400 398 396 394 392 390
80 78 76 74 72 70 68

FIG. 1

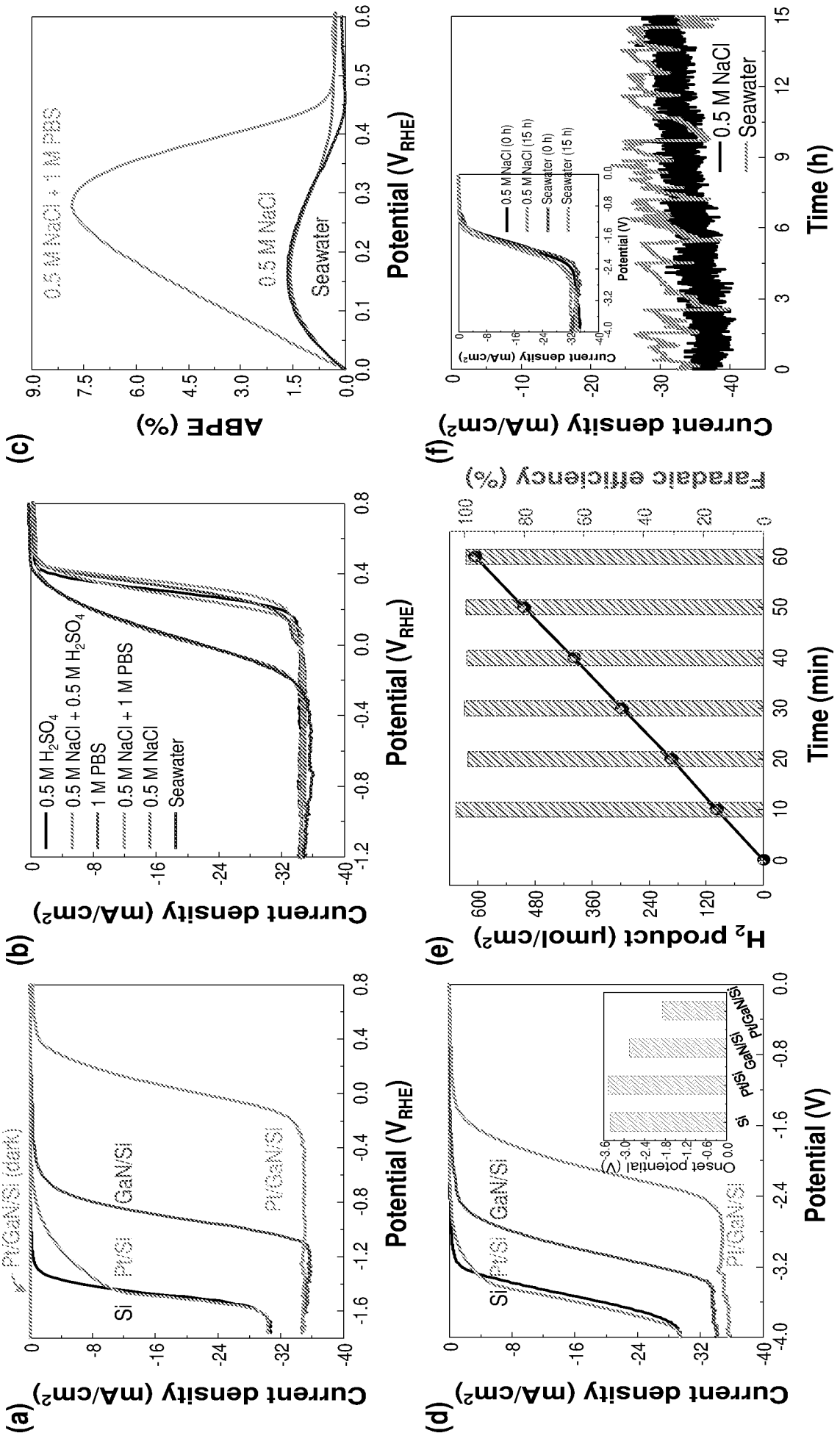
(a)
Current density (mA/cm²)
Potential (V_RHE)
Pt/GaN/Si (dark)
Si
Pt/Si
GaN/Si
Pt/GaN/Si
(b)
Current density (mA/cm²)
Potential (V_RHE)
0.5 M H2SO4
0.5 M NaCl + 0.5 M H2SO4
1 M PBS
0.5 M NaCl + 1 M PBS
0.5 M NaCl
Seawater
(c)
ABPE (%)
0.5 M NaCl + 1 M PBS
0.5 M NaCl
Seawater
(d)
Current density (mA/cm²)
Potential (V)
Si
Pt/Si
GaN/Si
Pt/GaN/Si
Onset potential (V)
Si
Pt/Si
GaN/Si
Pt/GaN/Si
(e)
H2 product (μmol/cm²)
Faradaic efficiency (%)
Time (min)
(f)
Current density (mA/cm²)
Time (h)
0.5 M NaCl (0 h)
0.5 M NaCl (15 h)
Seawater (0 h)
Seawater (15 h)
Potential (V)
0.5 M NaCl
Seawater

FIG. 2

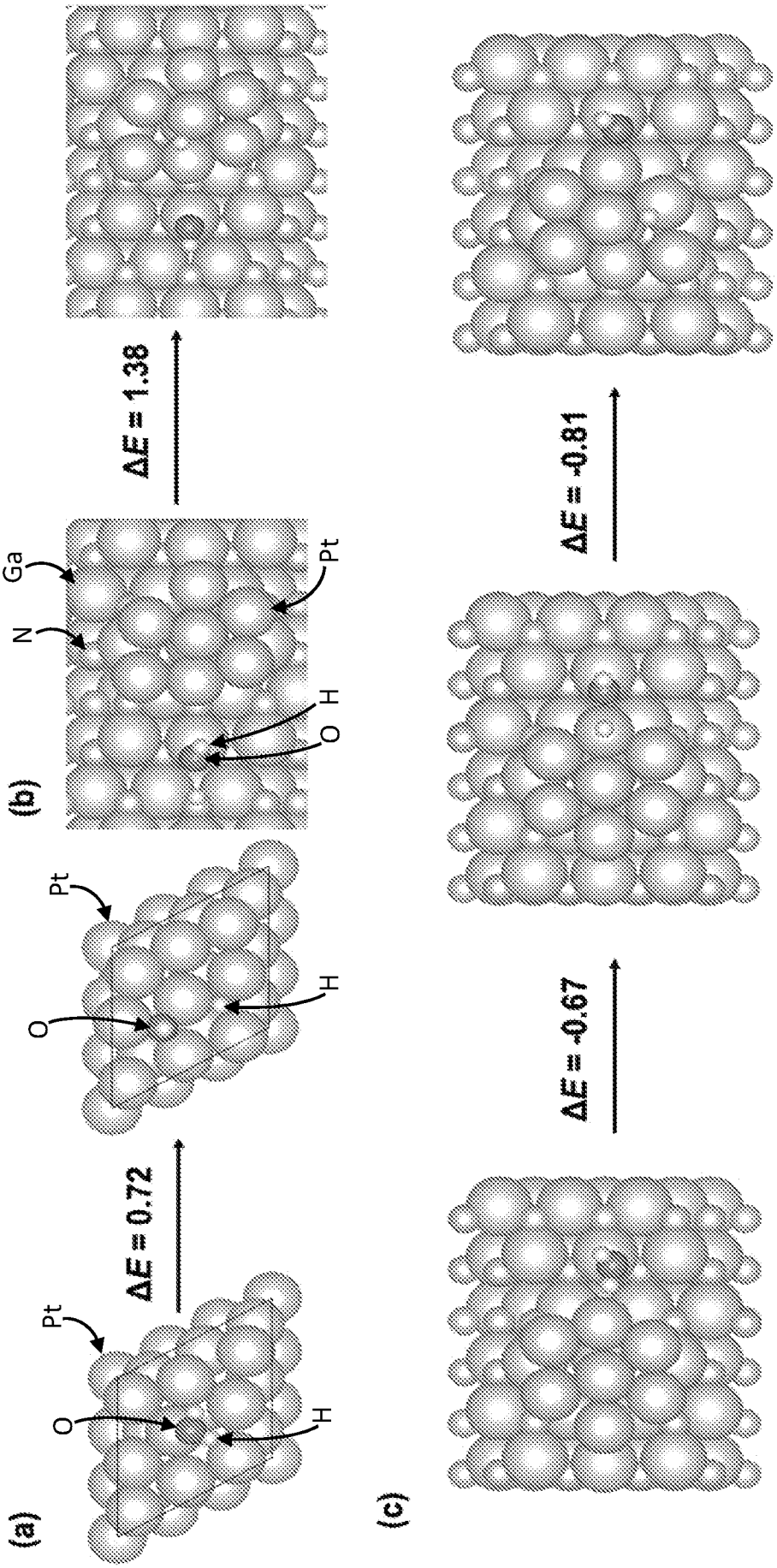

FIG. 3

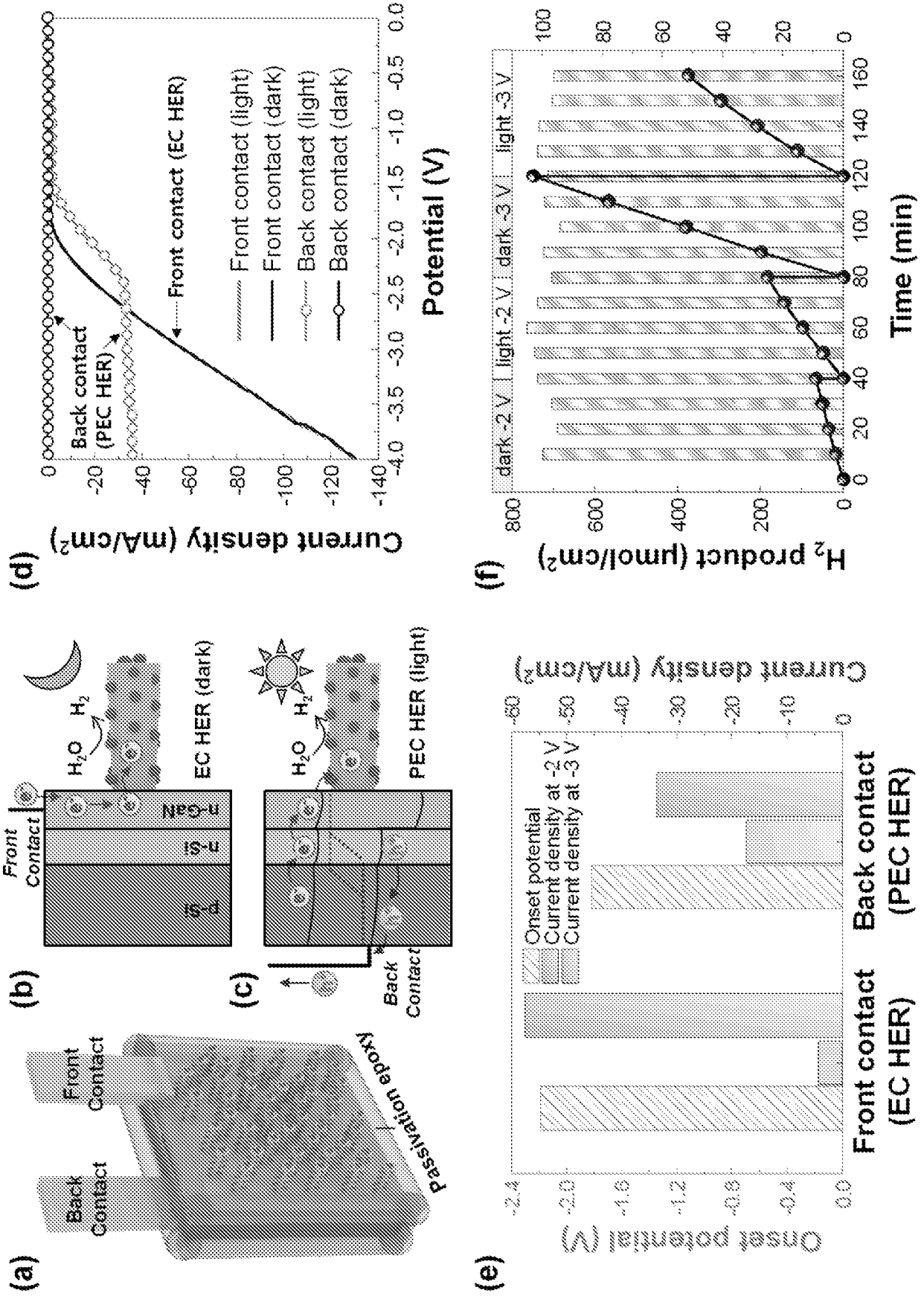
(a)
Back Contact
Front Contact
Passivation epoxy
(b)
Front Contact
p-Si
n-Si
n-GaN
H_2O
H_2
EC HER (dark)
(c)
Back Contact
PEC HER (light)
(d)
Current density (mA/cm²)
Potential (V)
Back contact (PEC HER)
Front contact (EC HER)
Front contact (light)
Front contact (dark)
Back contact (light)
Back contact (dark)
(e)
Onset potential (V)
Current density (mA/cm²)
Onset potential
Current density at -2 V
Current density at -3 V
Front contact (EC HER)
Back contact (PEC HER)
(f)
H_2 product (μmol/cm²)
Faradaic efficiency (%)
Time (min)
dark -2 V
light -2 V
dark -3 V
light -3 V

FIG. 4

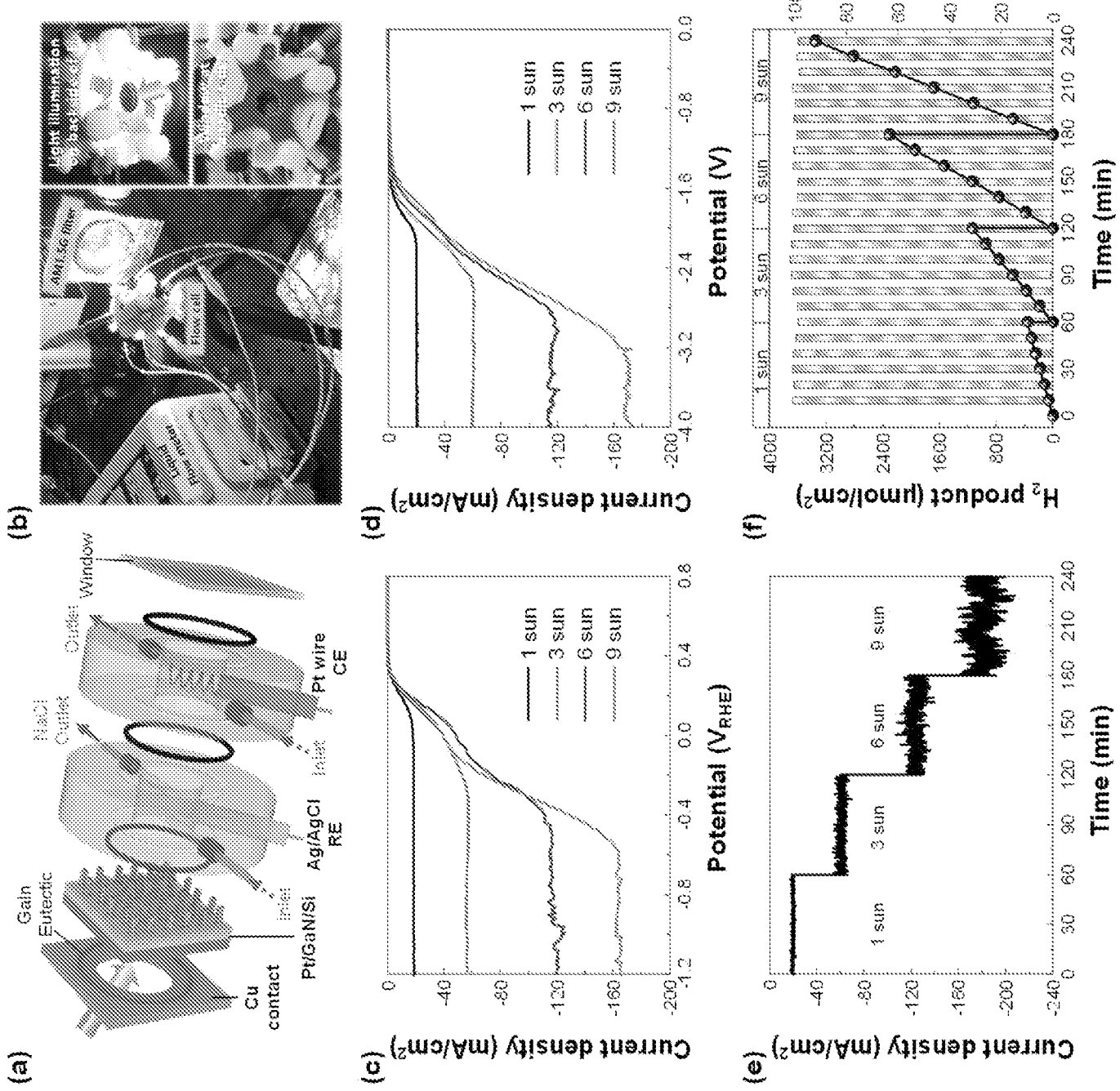
(a)
Gain Eutectic
Cu contact
Pt/GaN/Si
Inlet
Ag/AgCl RE
NaCl Outlet
Outlet
Window
Pt wire CE
(b)
Matrix fiber
Flow cell
Solar illumination
(c)
Current density (mA/cm²)
Potential (V_RHE)
1 sun
3 sun
6 sun
9 sun
(d)
Current density (mA/cm²)
Potential (V)
1 sun
3 sun
6 sun
9 sun
(e)
Current density (mA/cm²)
Time (min)
1 sun
3 sun
6 sun
9 sun
(f)
H₂ product (μmol/cm²)
Faradaic efficiency (%)
Time (min)
1 sun
3 sun
6 sun
9 sun

FIG. 5

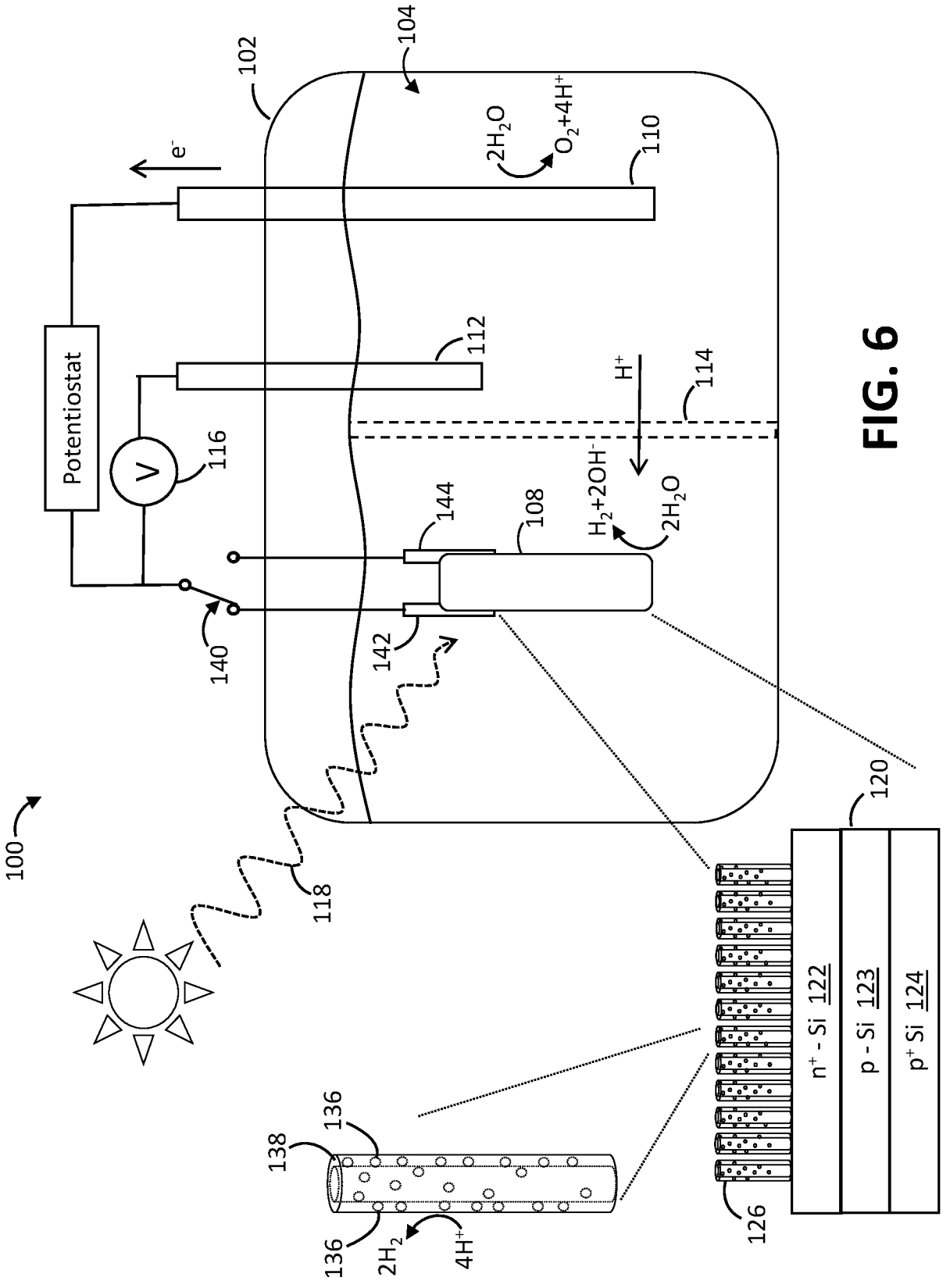
100
102
104
110
112
114
116
118
120
122
123
124
126
136
138
140
142
144
108
Potentiostat
V
e⁻
2H2O
O2+4H+
H+
H2+2OH⁻
2H2O
2H2
4H+
n+ - Si
p - Si
p+ Si

FIG. 6

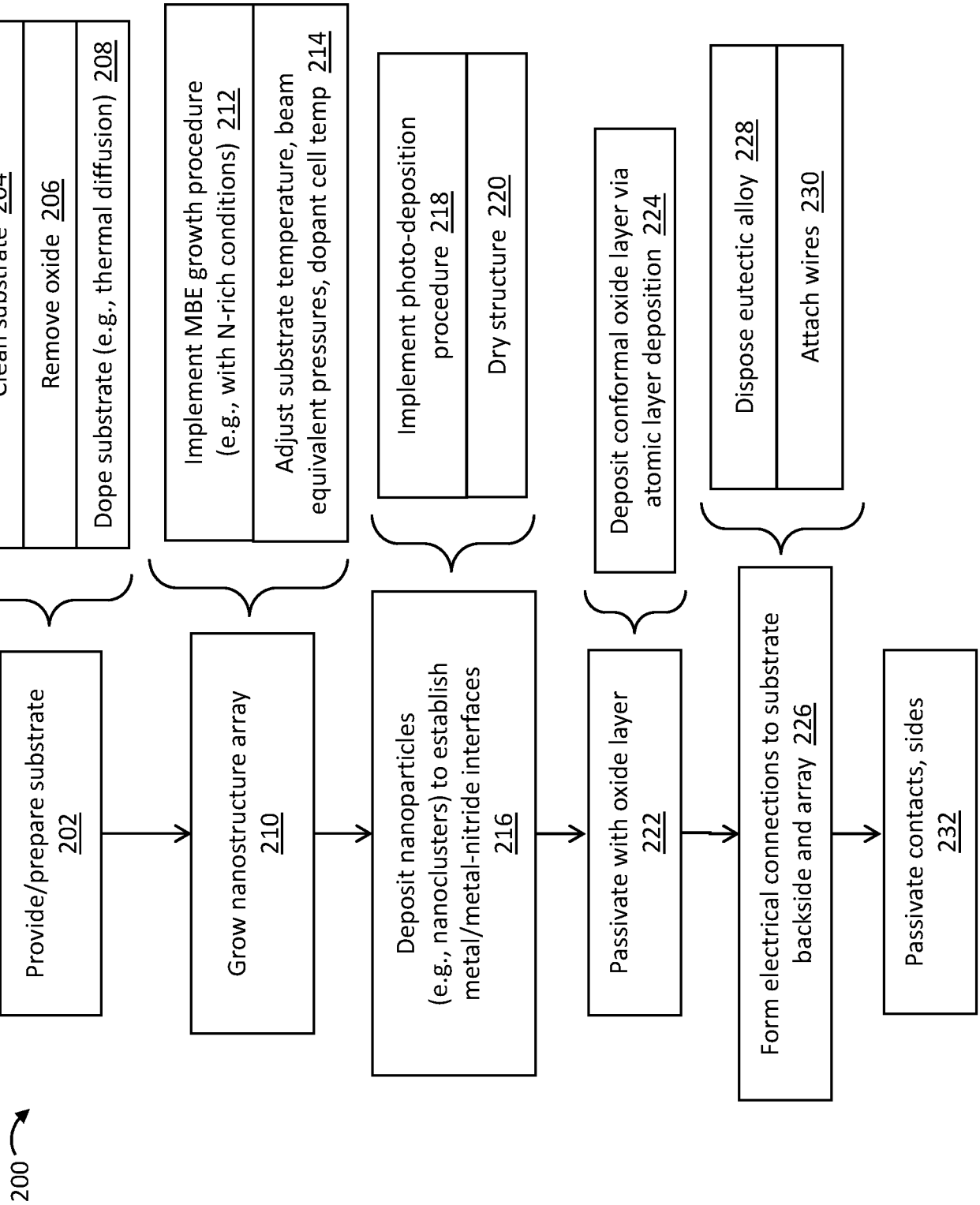
200
Provide/prepare substrate 202
Clean substrate 204
Remove oxide 206
Dope substrate (e.g., thermal diffusion) 208
Grow nanostructure array 210
Implement MBE growth procedure (e.g., with N-rich conditions) 212
Adjust substrate temperature, beam equivalent pressures, dopant cell temp 214
Deposit nanoparticles (e.g., nanoclusters) to establish metal/metal-nitride interfaces 216
Implement photo-deposition procedure 218
Dry structure 220
Passivate with oxide layer 222
Deposit conformal oxide layer via atomic layer deposition 224
Form electrical connections to substrate backside and array 226
Dispose eutectic alloy 228
Attach wires 230
Passivate contacts, sides 232

FIG. 7

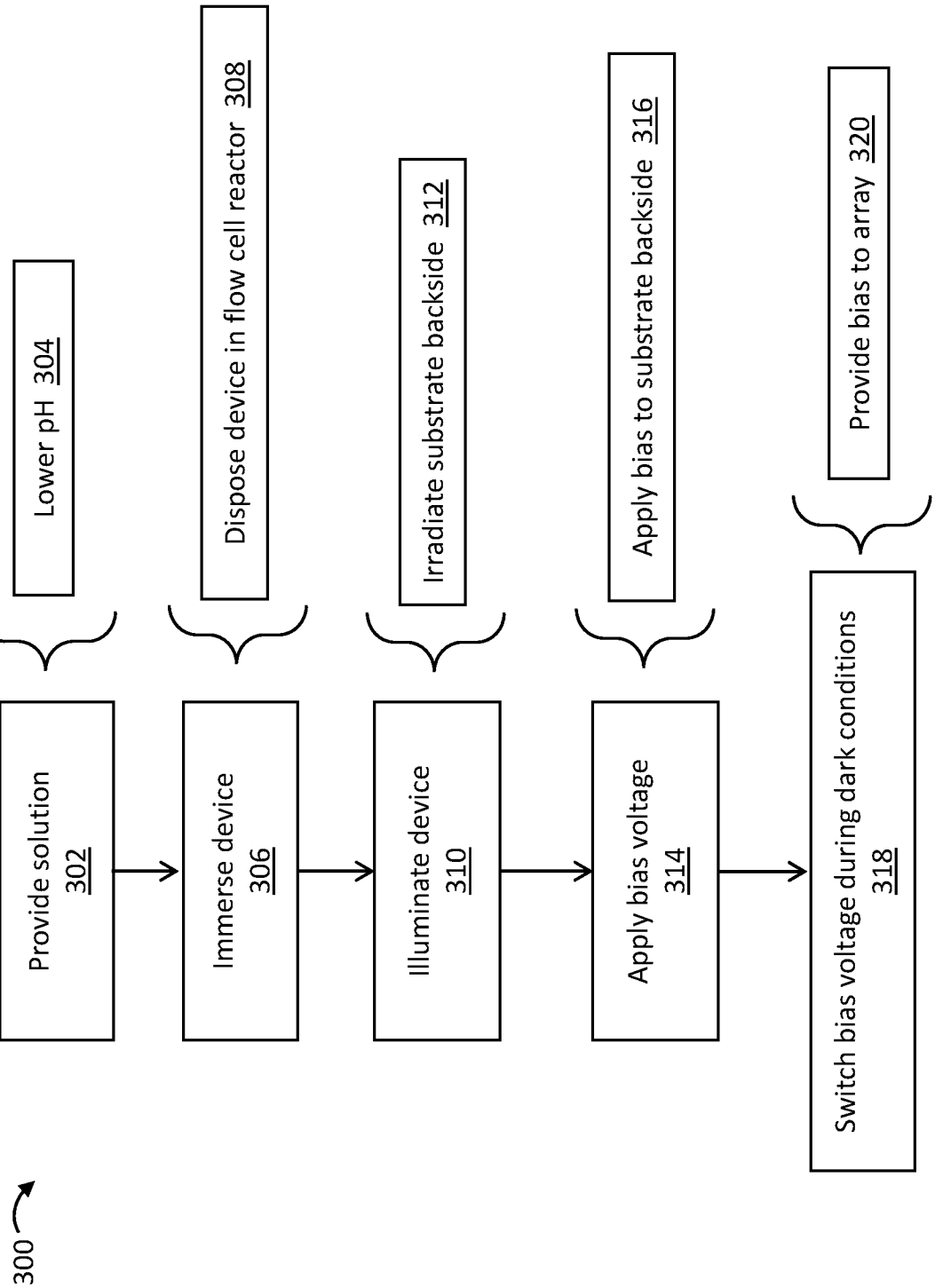
300
Provide solution 302
Lower pH 304
Immerse device 306
Dispose device in flow cell reactor 308
Illuminate device 310
Irradiate substrate backside 312
Apply bias voltage 314
Apply bias to substrate backside 316
Switch bias voltage during dark conditions 318
Provide bias to array 320

FIG. 8